bioRxiv preprint doi: https://doi.org/10.1101/2021.09.28.462275; this version posted August 9, 2022. The copyright holder for this preprint (which was not certified by peer review) is the author/funder, who has granted bioRxiv a license to display the preprint in perpetuity. It is made available under aCC-BY 4.0 International license.

1 **Bcr4 is a Chaperone for the Inner Rod Protein in the *Bordetella* Type III Secretion**
2 **System**
3
4 Masataka Goto[a], Akio Abe[a], Tomoko Hanawa[b], Masato Suzuki[c], and Asaomi Kuwae[a#]
5
6 [a]Laboratory of Bacterial Infection, Graduate School of Infection Control Sciences, Kitasato
7 University, Tokyo, Japan
8 [b]Department of Infectious Diseases, Kyorin University School of Medicine, Tokyo, Japan
9 [c]Antimicrobial Resistance Research Center, National Institute of Infectious Diseases, Tokyo,
10 Japan
11
12
13 **Running Head:** Bcr4 is a Chaperone for Inner Rod in *Bordetella* T3SS
14
15 [#]**Address Correspondence to:** Asaomi Kuwae, kuwae@lisci.kitasato-u.ac.jp
16
17
18
19
20

bioRxiv preprint doi: https://doi.org/10.1101/2021.09.28.462275; this version posted August 9, 2022. The copyright holder for this preprint (which was not certified by peer review) is the author/funder, who has granted bioRxiv a license to display the preprint in perpetuity. It is made available under aCC-BY 4.0 International license.

21 **Abstract**

22 *Bordetella bronchiseptica* injects virulence proteins called effectors into host cells via a
23 type III secretion system (T3SS) conserved among many Gram-negative bacteria. Small
24 proteins called chaperones are required for stabilizing some T3SS components or
25 localizing them to the T3SS machinery. In a previous study, we identified a chaperone-like
26 protein named Bcr4 that regulates T3SS activity in *B. bronchiseptica*. Bcr4 does not show
27 strong sequence similarity to well-studied T3SS proteins of other bacteria, and its function
28 remains to be elucidated. Here, we investigated the mechanism by which Bcr4 controls
29 T3SS activity. A pull-down assay revealed that Bcr4 interacts with BscI, based on its
30 homology to other bacterial proteins, to be an inner rod protein of the T3SS machinery. An
31 additional pull-down assay using truncated Bcr4 derivatives and secretion profiles of *B.*
32 *bronchiseptica* producing truncated Bcr4 derivatives showed that the Bcr4 C-terminal
33 region is necessary for the interaction with BscI and activation of the T3SS. Moreover, the
34 deletion of BscI abolished the secretion of type III secreted proteins from *B. bronchiseptica*
35 and the translocation of a cytotoxic effector into cultured mammalian cells. Finally, we
36 showed that BscI is unstable in the absence of Bcr4. These results suggest that Bcr4
37 supports the construction of the T3SS machinery by stabilizing BscI. This is the first
38 demonstration of a chaperone for the T3SS inner rod protein among the virulence bacteria
39 possessing the T3SS.

40

bioRxiv preprint doi: https://doi.org/10.1101/2021.09.28.462275; this version posted August 9, 2022. The copyright holder for this preprint (which was not certified by peer review) is the author/funder, who has granted bioRxiv a license to display the preprint in perpetuity. It is made available under aCC-BY 4.0 International license.

41

bioRxiv preprint doi: https://doi.org/10.1101/2021.09.28.462275; this version posted August 9, 2022. The copyright holder for this preprint (which was not certified by peer review) is the author/funder, who has granted bioRxiv a license to display the preprint in perpetuity. It is made available under aCC-BY 4.0 International license.

42 **Importance**

43 The type III secretion system (T3SS) is a needle-like complex that projects outward from
44 bacterial cells. *Bordetella bronchiseptica* uses the T3SS to inject virulence proteins into
45 host cells. Our previous study reported that a protein named Bcr4 is essential for the
46 secretion of virulence proteins from *B. bronchiseptica* bacterial cells and delivery through
47 the T3SS. Because other bacteria lack a Bcr4 homologue, the function of Bcr4 has not
48 been elucidated. In this study, we discovered that Bcr4 interacts with BscI, a component of
49 the T3SS machinery. We showed that a *B. bronchiseptica* BscI-deficient strain was unable
50 to secrete type III secreted proteins. Furthermore, in a *B. bronchiseptica* strain that
51 overproduces T3SS component proteins, Bcr4 is required to maintain BscI in bacterial cells.
52 These results suggest that Bcr4 stabilizes BscI to allow construction of the T3SS in *B.*
53 *bronchiseptica*.
54
55
56
57
58
59
60
61
62

63

bioRxiv preprint doi: https://doi.org/10.1101/2021.09.28.462275; this version posted August 9, 2022. The copyright holder for this preprint (which was not certified by peer review) is the author/funder, who has granted bioRxiv a license to display the preprint in perpetuity. It is made available under aCC-BY 4.0 International license.

64 **Introduction**

65 The genus *Bordetella* consists of Gram-negative bacteria that infect the respiratory tracts
66 of mammals including humans. *Bordetella pertussis* causes a severe coughing attack
67 called whooping cough in humans (1, 2). *Bordetella bronchiseptica* causes atrophic rhinitis
68 in pigs and kennel cough in dogs (1, 2). These *Bordetella* spp. harbor a virulence factor
69 secretion apparatus called the type III secretion system (T3SS).

70 The T3SS consists of a basal body that penetrates the inner and outer membranes of the
71 bacteria and a needle structure that protrudes outside the bacteria, and is conserved in
72 many Gram-negative bacteria such as *Yersinia*, *Salmonella*, and *Pseudomonas*. *B.*
73 *bronchiseptica* uses the T3SS to inject virulence factors, called effectors, into host cells to
74 disrupt the physiological functions of host cells (3). Once the basal body and the export
75 apparatus of the T3SS are completed, the type III secreted proteins are secreted in a fixed
76 order. First, the components (Table S1) of the needle structure (SctF) and the inner rod
77 (SctI) that ties the needle structure to the basal body are secreted. After the needle is
78 completed, translocators (SctE and SctB) are secreted, which form small pores in the host
79 cell membrane to create a pathway for effectors. Finally, the effectors translocate into the
80 host cell via the T3SS (4, 5). In *B. bronchiseptica*, BopB (SctE) (6), BopD (SctB) (7), and
81 Bsp22 (SctA) (8) function as translocators (Table S1), while BteA (also referred to as BopC)
82 (9, 10), BopN (11, 12), and BspR (also referred to as BtrA) (13, 14) function as effectors.
83 Bsp22 is located at the tip of the needle and bridges the needle to the pore-forming factors

bioRxiv preprint doi: https://doi.org/10.1101/2021.09.28.462275; this version posted August 9, 2022. The copyright holder for this preprint (which was not certified by peer review) is the author/funder, who has granted bioRxiv a license to display the preprint in perpetuity. It is made available under aCC-BY 4.0 International license.

84 embedded in the plasma membrane (15). BteA has been shown to cause
85 membrane-disrupting cytotoxicity in mammalian cells (10). BspR is a regulator that
86 represses transcription of the *bteA* gene and genes on the *bsc* locus (Fig. S1), where genes
87 encoding type III secreted proteins and components of T3SS are located (14, 16).
88 According to secondary structure prediction—e.g., the predicted positions of helix, and the
89 overall structure of the operon—the BscF and BscI of *B. bronchiseptica* correspond to
90 *Yersinia* needle YscF (SctF) and inner rod YscI (SctI), respectively (Table S1).

91 In addition, many type III secreted proteins have unique chaperones that are involved in
92 stabilizing the substrate and preventing premature polymerization of the substrate in the
93 bacterial cytosol, and then in efficiently transporting the substrate to the T3SS machinery
94 (17-20). For example, PscE and PscG function as chaperones of the needle PscF (SctF) in
95 *Pseudomonas* (Table S1). These chaperones stabilize PscF in the bacterial cytosol and are
96 involved in PscF secretion through the T3SS (21). In bacteria such as *Yersinia* and
97 *Pseudomonas*, an inner rod chaperone is thought to exist, because the inner rod is
98 secreted out of the bacterial cell and polymerized (22, 23). However, a chaperone for the
99 inner rod has not been reported.

100 So far, a chaperone-like protein called Bcr4 has been identified in *B. bronchiseptica* (24).
101 *Bordetella* Bcr4 is highly conserved among *B. pertussis*, *B. parapertussis*, and *B.*
102 *bronchiseptica* (Fig. S2). In this study, we attempted to identify factors that interact with
103 Bcr4 in order to investigate how Bcr4 is involved in the T3SS regulation.

bioRxiv preprint doi: https://doi.org/10.1101/2021.09.28.462275; this version posted August 9, 2022. The copyright holder for this preprint (which was not certified by peer review) is the author/funder, who has granted bioRxiv a license to display the preprint in perpetuity. It is made available under aCC-BY 4.0 International license.

104 **Results**

105 **Bcr4 binds to BscI, an inner rod protein of the *Bordetella* type III secretion system.**

106 The results of a previous study suggested that Bcr4 is a chaperone for components of the
107 type III secretion system (T3SS) (24). T3SS chaperones are known to be involved in
108 substrate stability and efficient transport of substrates to the T3SS machinery (17, 19, 20).
109 In addition, it is generally known that the genes of these chaperones are localized adjacent
110 to genes encoding their substrates (25). On the *B. bronchiseptica* S798 chromosome, the
111 genes encoding BcrH2, BscI, BscJ, and BscK are located in the vicinity of the *bcr4* gene
112 (Fig. 1A), and these proteins are predicted to function as a translocator chaperone, inner
113 rod (SctI), inner membrane ring (SctJ), and ATPase cofactor (SctK), respectively (Table S1)
114 (5, 26). To test whether Bcr4 binds to BscI, BscJ or BscK, we added *E. coli* lysates
115 containing the V5-tagged target proteins (BscI-V5, BscJ-V5 or BscK-V5) to Strep-Tactin
116 beads loaded with the purified Strep-tagged Bcr4 (Bcr4-Strep), and then performed the
117 pull-down assay. The supernatant fraction (Sup) and pellet fraction (Pellet) samples were
118 prepared, separated by SDS-PAGE, and subjected to Western blotting with anti-V5
119 antibody (Fig. 1B). When the beads were washed with TBS, the V5 signal of the BscI-V5
120 pellet sample was detected in the beads loaded with Bcr4, but not in the unloaded beads
121 (Fig. 1B). The V5 signals of the BscK-V5 and BscJ-V5 pellet samples were detected in both
122 the Bcr4-loaded beads and the unloaded beads when washed with TBS, and not detected
123 when washed with TBS containing 0.1% Triton X-100 (Fig. 1B). These results suggest that

bioRxiv preprint doi: https://doi.org/10.1101/2021.09.28.462275; this version posted August 9, 2022. The copyright holder for this preprint (which was not certified by peer review) is the author/funder, who has granted bioRxiv a license to display the preprint in perpetuity. It is made available under aCC-BY 4.0 International license.

124 Bcr4 binds to BscI, an inner rod protein of the *Bordetella* T3SS.

125 Next, to confirm that Bcr4 binds to BscI, a pull-down assay was performed by adding *E.*
126 *coli* lysate containing V5-tagged Bcr4 (Bcr4-V5) to Strep-Tactin beads with the purified
127 Strep-tagged BscI (BscI-Strep) or BteA N-terminal 1–312 amino acids region
128 (BteA-N-Strep). BteA is a protein secreted from the type III secretion system and interacts
129 with its cognate chaperone BtcA through the N-terminal (9). As a result, the V5 signal was
130 detected in the pellet sample of the BscI-Strep, but was hardly detected in that of the
131 BteA-N-Strep (Fig. 1C). These results strongly suggested that Bcr4 binds to BscI.

132

133 **The C-terminal region of Bcr4 is required for the binding of Bcr4 to BscI.**

134 Next, to investigate the Bcr4 region responsible for the binding to BscI, we
135 produced Strep-tagged full-length Bcr4 (Bcr4-FL-Strep), Bcr4 lacking amino acids region
136 58–109 (Bcr4Δ58-109-Strep), and Bcr4 lacking amino acids region 110–173
137 (Bcr4Δ110-173-Strep) in *E. coli* (Fig. 2A). A pull-down assay was performed by adding *E.*
138 *coli* lysate containing V5-tagged BscI (BscI-V5) to Strep-Tactin beads with the purified
139 Bcr4-FL-Strep, Bcr4Δ58-109-Strep, or Bcr4Δ110-173-Strep. The Sup and Pellet samples
140 were then prepared, separated by SDS-PAGE, and subjected to Western blotting using
141 anti-V5 antibody (Fig. 2B). As a result, the V5 signal was detected in the pellet sample of
142 Bcr4-FL-Strep, but not in those of Bcr4Δ58-109-Strep and Bcr4Δ110-173-Strep. Although it
143 is still unknown which region of Bcr4 directly interacts with BscI, our results strongly

bioRxiv preprint doi: https://doi.org/10.1101/2021.09.28.462275; this version posted August 9, 2022. The copyright holder for this preprint (which was not certified by peer review) is the author/funder, who has granted bioRxiv a license to display the preprint in perpetuity. It is made available under aCC-BY 4.0 International license.

144 suggest that both the Bcr4-58-109 and Bcr4-110-173 regions are required for the
145 interaction.
146

147 **The C-terminal region of Bcr4 is required for T3SS activity.**

148 The results in Figure 2 suggest that the C-terminal region of Bcr4 is required for binding
149 to BscI. Therefore, we introduced plasmids encoding the full-length FLAG-tagged Bcr4
150 (Bcr4-FL-FLAG), Bcr4 with the 5 C-terminal amino acids deleted (Bcr4Δ169-173-FLAG),
151 Bcr4 with the 10 C-terminal amino acids deleted (Bcr4Δ164-173-FLAG), and Bcr4 with the
152 15 C-terminal amino acids deleted (Bcr4Δ159-173-FLAG) (Fig. 3 A) into a Bcr4-deficient
153 strain (Δ*bcr4*) (Δ*bcr4*+*bcr4*-FL-FLAG, Δ*bcr4*+*bcr4*Δ169-173-FLAG,
154 Δ*bcr4*+*bcr4*Δ164-173-FLAG and Δ*bcr4*+*bcr4*Δ159-173-FLAG, respectively). Whole cell
155 lysates (WCL) and culture supernatant fraction (CS) samples were prepared from these
156 strains and separated by SDS-PAGE. Western blottings were then carried out using
157 antibodies against Bcr4, FLAG, BteA (an effector and a type III secreted protein), BopD
158 (SctB, a translocator and a type III secreted protein) or RpoB (an internal control of WCL)
159 (Fig. 3B). Since the antibody against Bcr4 was generated using its 18 C-terminal amino
160 acids (amino acids (aa) 156–173) as the antigen peptide, we considered that it may not
161 recognize the Bcr4 partial deletion mutant proteins used in this experiment. Therefore, we
162 also performed Western blotting using anti-FLAG antibody (Fig. 3B). As a result, when
163 anti-Bcr4 antibody was used against the WCL samples, signals were detected in the

bioRxiv preprint doi: https://doi.org/10.1101/2021.09.28.462275; this version posted August 9, 2022. The copyright holder for this preprint (which was not certified by peer review) is the author/funder, who has granted bioRxiv a license to display the preprint in perpetuity. It is made available under aCC-BY 4.0 International license.

164 wild-type, Δ*bcr4*+*bcr4*-FL-FLAG and Δ*bcr4*+*bcr4* Δ169-173-FLAG, but almost no signals
165 were detected in Δ*bcr4*+*bcr4*Δ164-173-FLAG and Δ*bcr4*+*bcr4*Δ159-173-FLAG (Fig. 3B).
166 On the other hand, when anti-FLAG antibody was used, signals were detected in
167 Δ*bcr4*+*bcr4*Δ164-173-FLAG and Δ*bcr4*+*bcr4*Δ159-173-FLAG (Fig. 3B). These results
168 confirmed that the Bcr4 partial deletion mutant proteins were produced in the Δ*bcr4* strain.
169 When anti-BteA or anti-BopD antibodies were used against the CS samples, signals were
170 detected in the wild-type, Δ*bcr4*+*bcr4*-FL-FLAG, Δ*bcr4*+*bcr4*Δ169-173-FLAG and
171 Δ*bcr4*+*bcr4*Δ164-173-FLAG, respectively, but not in Δ*bcr4* or Δ*bcr4*+*bcr4*Δ159-173-FLAG
172 (Fig. 3B). We attempted to create *B. bronchiseptica* strains that produce shorter Bcr4, e.g.
173 amino acid regions 1-57, 58-109, and 110-173, however, those truncated Bcr4 were
174 produced at very low levels (data not shown). Therefore, we were unable to evaluate
175 whether or not these truncated proteins were functional in *B. bronchiseptica*. We then
176 infected L2 cells (a rat lung epithelial cell line) with the wild-type, Δ*bcr4*,
177 Δ*bcr4*+*bcr4*-FL-FLAG, Δ*bcr4*+*bcr4*Δ169-173-FLAG, Δ*bcr4*+*bcr4*Δ164-173-FLAG or
178 Δ*bcr4*+*bcr4*Δ159-173-FLAG strain at a multiplicity of infection (MOI) of 50 for 1 h and
179 measured the amounts of LDH released into the culture medium as an index of cytotoxicity.
180 As a result, LDH was detected in the medium of cells infected with Δ*bcr4*+*bcr4*-FL-FLAG,
181 Δ*bcr4*+*bcr4*Δ169-173-FLAG or Δ*bcr4*+*bcr4*Δ164-173-FLAG, but not in the medium of cells
182 infected with Δ*bcr4*+*bcr4*Δ159-173-FLAG (Fig. 3C). These results suggest that the region
183 required for the T3SS function is located in the 159–163 amino acids region of Bcr4.

bioRxiv preprint doi: https://doi.org/10.1101/2021.09.28.462275; this version posted August 9, 2022. The copyright holder for this preprint (which was not certified by peer review) is the author/funder, who has granted bioRxiv a license to display the preprint in perpetuity. It is made available under aCC-BY 4.0 International license.

184

185 **BscI is required for the function of the T3SS in *B. bronchiseptica*.**

186 BscI is a homologue of YscI, an inner rod (SctI) of the *Yersinia* T3SS, and YscI is
187 essential for the function of the T3SS (22). To confirm that BscI is required for the function
188 of the *B. bronchiseptica* T3SS, the *B. bronchiseptica* S798 wild-type, BscI-deficient strain
189 (Δ*bscI*), BscI-complemented strain (Δ*bscI*+*bscI*), and BscN-deficient strain (Δ*bscN*) were
190 cultured in SS medium. BscN is a protein predicted to function as an ATPase (SctN) and is
191 required for the T3SS function in *Bordetella bronchiseptica* (Table S1) (6, 27). We used the
192 Δ*bscN* as a T3SS-deficient strain. WCL and CS samples were prepared, and these
193 samples were separated by SDS-PAGE and analyzed by Western blotting using antibodies
194 against BscI, BteA, BopD, Bsp22 (SctA, a translocator and a component of the filament-like
195 structure; Fig. 7) or FHA (filamentous hemagglutinin, an adhesion factor) (Fig. 4A). As
196 expected, the FHA signals were detected in the WCL and CS samples of all strains used
197 here (Fig. 4A). In contrast, no signals of BscI were detected in the WCL samples of all
198 strains used here (Fig. 4A). The BscI signal was detected in the CS of Δ*bscI*+*bscI*, and a
199 faint BscI signal was detected in the CS of the wild-type (Fig. 4A). In order to examine
200 whether the signal we obtained around 20 kDa in the western blot using anti-BscI antibody
201 in Fig. 4A was specific or nonspecific, we prepared the supernatant fraction from Δ*bsp22*
202 strain. As a result, the signal disappeared in the supernatant fraction of the Δ*bsp22* strain
203 (Fig. S3), suggesting that the signal around 20 kDa obtained in the western blot was a

bioRxiv preprint doi: https://doi.org/10.1101/2021.09.28.462275; this version posted August 9, 2022. The copyright holder for this preprint (which was not certified by peer review) is the author/funder, who has granted bioRxiv a license to display the preprint in perpetuity. It is made available under aCC-BY 4.0 International license.

204 nonspecific interaction between anti-BscI antibody and an excess amount of Bsp22 on the
205 membrane. The BteA, BopD and Bsp22 signals were detected in the CS of the wild-type
206 and Δ*bscI*+*bscI*, but not in those of Δ*bscI* and Δ*bscN* (Fig. 4A). BspR is a negative regulator
207 that represses the transcription of genes on the *bsc* locus (14). In *Bordetella* strains that are
208 unable to secrete type III secreted proteins, such as Bcr4-deficient strains (Δ*bcr4*), the
209 repression of the *bsc* locus transcriptions by BspR is enhanced (24). Therefore, we
210 speculated that the production of BopD and Bsp22 was intensely suppressed by BspR in
211 Δ*bscI* due to the loss of T3SS activity. To test whether this hypothesis is correct, we
212 generated Δ*bspR*Δ*bscI* (a BspR- and BscI-deficient strain). WCL and CS samples were
213 prepared from the *B. bronchiseptica* S798 wild-type strain, Δ*bspR*, Δ*bspR*Δ*bscI* or
214 Δ*bspR*Δ*bscI*+*bscI* (BscI-complemented BspR- and BscI-deficient strain), and these
215 samples were separated by SDS-PAGE and analyzed by Western blotting using antibodies
216 against Bsp22 or BopB (SctE, a translocator and a type III secreted protein). As a result, the
217 Bsp22 and BopB signals were detected in the WCL samples of the wild-type, Δ*bspR*,
218 Δ*bspR*Δ*bscI* and Δ*bspR*Δ*bscI*+*bscI* strains (Fig. 4B). The Bsp22 and BopB signals were
219 detected in the CS samples of the wild-type, Δ*bspR* and Δ*bspR*Δ*bscI*+*bscI* strains, but not
220 in that of the Δ*bspR*Δ*bscI* strain (Fig. 4B). These results suggest that in *B. bronchiseptica*,
221 BscI is required for the function of the T3SS and is secreted out of the bacterial cell.
222

223 **BscI plays an important role in the function of the *B. bronchiseptica* T3SS during**

bioRxiv preprint doi: https://doi.org/10.1101/2021.09.28.462275; this version posted August 9, 2022. The copyright holder for this preprint (which was not certified by peer review) is the author/funder, who has granted bioRxiv a license to display the preprint in perpetuity. It is made available under aCC-BY 4.0 International license.

224 **infection of cultured mammalian cells.**

225 To further investigate whether BscI is required for the construction and function of the T3SS
226 in *B. bronchiseptica*, we infected L2 cells with the wild-type, Δ*bscI*, Δ*bscI*+*bscI* or Δ*bscN*
227 and measured the number of Bsp22 (SctA, a translocator, and a component of the
228 filament-like structure; Fig. 5) signals detected on L2 cells by immunofluorescence
229 microscopy. For the efficient detection of Bsp22 signals, we cultured the bacteria in
230 iron-depleted SS medium, which has been shown to increase the amount of type III
231 secreted protein secreted by *B. bronchiseptica* (28). L2 cells were infected with bacteria for
232 1 h at an MOI of 2000. Then, Bsp22, F-actin and bacteria were stained with anti-Bsp22
233 antibody, Rhodamine-Phalloidin and DAPI, respectively (Fig. 5A). The DAPI fluorescence
234 signals showing bacterial genomic DNA were detected to the same extent among the L2
235 cells infected with each bacterial strain, suggesting that the amounts of each mutant
236 adhered to the cells were not significantly reduced when compared to the wild-type strain
237 (Fig. 5A). The fluorescence signals of Bsp22 were detected on the L2 cells infected with the
238 wild-type or Δ*bscI*+*bscI*, but not on the L2 cells infected with Δ*bscI* or Δ*bscN* (Fig. 5 A, B).
239 We also infected L2 cells with the wild-type, Δ*bscI*, Δ*bscI*+*bscI* or Δ*bscN* for 1 h at an MOI of
240 200 and measured the amount of LDH released into the extracellular medium. The results
241 showed that LDH was detected in the medium of L2 cells infected with the wild-type or
242 Δ*bscI*+*bscI*, but not in the medium of L2 cells infected with Δ*bscI* or Δ*bscN* (Fig. 5 C). These

bioRxiv preprint doi: https://doi.org/10.1101/2021.09.28.462275; this version posted August 9, 2022. The copyright holder for this preprint (which was not certified by peer review) is the author/funder, who has granted bioRxiv a license to display the preprint in perpetuity. It is made available under aCC-BY 4.0 International license.

243 results suggest that BscI is required for the construction of the T3SS and induction of
244 T3SS-dependent death of mammalian cells in *B. bronchiseptica*.
245

246 **Bcr4 is required for the stability of BscI and is suggested to interact with BscI in *B.***
247 ***bronchiseptica*.**

248 As mentioned above, our results suggested that Bcr4 interacts with BscI (Fig. 1). Because
249 Bcr4 has various properties like those of chaperones for the type III secreted proteins (25),
250 e.g., low molecular mass (18.1 kDa) and low isoelectric point (pI 4.41), we investigated
251 whether Bcr4 is involved in the stability of BscI. We cultured the *B. bronchiseptica* wild-type,
252 Bcr4-deficient strain (Δ*bcr4* , T3SS-inactive strain) (24), BspR-deficient strain (Δ*bspR* ,
253 T3SS-overproducing and -oversecreting strain) (14) or BspR- and Bcr4-deficient strain
254 (Δ*bspR* , a T3SS-overproducing but -inactive strain) (24) in SS medium. The prepared WCL
255 samples were separated by SDS-PAGE, and Western blotting was performed using
256 antibodies against BscI, BscJ (SctJ, a protein composing the inner membrane ring of the
257 T3SS), or Bcr4. As shown in Fig. S1, the negative regulatory function of BspR, which
258 represses the *bsc* locus transcription, is enhanced in the strain that loses the activity
259 of T3SS, e.g., Δ*bcr4* (24). Because of this property of BspR, the BscJ signal of the WCL
260 sample was weaker in Δ*bcr4* than in the wild-type (Fig. 6A). In Δ*bspR* and Δ*bspR*Δ*bcr4*,
261 BscJ signals of the WCL samples were more strongly detected when compared to the
262 wild-type (Fig. 6A) due to the BspR deficiency. On the other hand, the BscI signals of the

bioRxiv preprint doi: https://doi.org/10.1101/2021.09.28.462275; this version posted August 9, 2022. The copyright holder for this preprint (which was not certified by peer review) is the author/funder, who has granted bioRxiv a license to display the preprint in perpetuity. It is made available under aCC-BY 4.0 International license.

263 WCL and CS samples were detected in Δ*bspR*, but not in the Δ*bspR*Δ*bcr4* strain (Fig. 6A).
264 To investigate the presence of *bscI* mRNA in Δ*bspR*Δ*bcr4*, a quantitative RT-PCR was
265 performed. The results showed that the amount of *bscI* mRNA in Δ*bspR*Δ*bcr4* was 1.5-fold
266 higher than that of *bscI* in Δ*bspR* (Fig. S4), demonstrating that the *bscI* gene is transcribed
267 in Δ*bspR*Δ*bcr4*. These results suggest that Bcr4 is necessary for the stability of BscI in *B.*
268 *bronchiseptica*. Finally, we examined whether Bcr4 binds to BscI inside of the *B.*
269 *bronchiseptica* cells. As described in the Discussion section, we were unable to detect an
270 interaction of Bcr4 with BscI by immunoprecipitation because of the low level of BscI protein
271 in bacterial cells. Therefore, we attempted to reveal the interaction by using a cross linker.
272 We treated the wild-type, Δ*bspR* and Δ*bspR*Δ*bcr4* strains with disuccinimidyl suberate
273 (DSS) and then prepared the whole cell lysate samples. The samples were separated by
274 SDS-PAGE and then analyzed by Western blotting using anti-Bcr4 antibody. As a result, an
275 extra signal around 33 kDa was evident in Δ*bspR* but not in Δ*bspR*Δ*bscI* (Fig. 6B). The size
276 of the extra signal was almost equivalent to that of the Bcr4-BscI complex, suggesting the
277 possibility that Bcr4 binds to BscI in the *B. bronchiseptica* cells.
278
279
280
281
282

bioRxiv preprint doi: https://doi.org/10.1101/2021.09.28.462275; this version posted August 9, 2022. The copyright holder for this preprint (which was not certified by peer review) is the author/funder, who has granted bioRxiv a license to display the preprint in perpetuity. It is made available under aCC-BY 4.0 International license.

283

284

bioRxiv preprint doi: https://doi.org/10.1101/2021.09.28.462275; this version posted August 9, 2022. The copyright holder for this preprint (which was not certified by peer review) is the author/funder, who has granted bioRxiv a license to display the preprint in perpetuity. It is made available under aCC-BY 4.0 International license.

285 **Discussion**

286 In the present study, we found that deletion of BscI in *B. bronchiseptica* abolished the
287 extracellular secretion of type III secreted proteins (Fig. 4, 5). In addition, when Bcr4 was
288 deleted in the *B. bronchiseptica* BspR-deficient strain, BscI (SctI, a protein composing the
289 inner rod of the *Bordetella* T3SS) was not detected in the bacterial cells (Fig. 6A). These
290 results suggest that Bcr4 contributes to the establishment of the T3SS in *B. bronchiseptica*
291 by stabilizing BscI (Fig. 7).

292 To date, chaperones for needles, translocators and effectors have been reported in
293 bacteria that retain the T3SS, such as *Yersinia* (29-32). However, a chaperone for the inner
294 rod protein has not been reported, and the mechanism underlying stability of the inner rod
295 in the bacterial cell and the transport of inner rods to the T3SS remain unclear.

296 In the present study, it was suggested that both the 58–109 and 110–173 amino acid
297 regions of Bcr4 are required for the binding of Bcr4 to BscI (Fig. 2B). To investigate whether
298 the 1–57 amino acids region of Bcr4 is also required for the binding of Bcr4 to BscI, we
299 attempted to purify Bcr4 lacking the N-terminal 1–57 amino acids region (Bcr4Δ1-57-Strep).
300 However, the amount of Bcr4Δ1-57-Strep produced in *E. coli* was extremely low (data not
301 shown), so a pull-down assay could not be performed. Figure 3B suggests that the 159–
302 163 amino acids region of Bcr4 is required for the function of the T3SS. However, it is still
303 unclear whether the 159−163 amino acids region of Bcr4 is required for binding to BscI.

bioRxiv preprint doi: https://doi.org/10.1101/2021.09.28.462275; this version posted August 9, 2022. The copyright holder for this preprint (which was not certified by peer review) is the author/funder, who has granted bioRxiv a license to display the preprint in perpetuity. It is made available under aCC-BY 4.0 International license.

304 Further analysis is needed to clarify whether the binding of Bcr4 to BscI is required for the
305 function of T3SS.

306 In this study, the BopD signal was detected in the WCL of the *B. bronchiseptica*
307 wild-type strain, but the BscI signal was not detected (Fig. 4A). We detected *bscI* mRNA in
308 *B. bronchiseptica*, and the amount of *bscI* mRNA was not less than that of *bopD* mRNA (Fig.
309 S5). Therefore, the amount of BscI protein present in *B. bronchiseptica* was considered to
310 be much lower than that of BopD. The reason for this finding is unknown, but it could be
311 due to the low efficiency of translation of the *bscI* gene. In order to detect BscI in the whole
312 cell lysate, we prepared the samples at 0 hr to 18 hr after suspending the bacteria in liquid
313 broth. However, no signals were detected in the whole cell lysate samples prepared from
314 the wild-type strain or the Δ*bcr4* strain (Fig. S6). We also used the Δ*bspR* and Δ*bspR*Δ*bcr4*
315 strains, and detected BscI signals in the Δ*bspR* strain, but not in the Δ*bspR*Δ*bcr4* double
316 knockout strain (Fig. S6), strongly suggesting that Bcr4 is important for the stability of BscI.

317 In this study, we attempted to detect the BscI signal using a BspR-deficient strain
318 (Δ*bspR*), in which the gene transcriptions on the *bsc* locus are promoted (Fig. 6), because
319 the BscI signal was not detected in the WCL sample of the *B. bronchiseptica* wild-type (Fig.
320 4). The *bscJ* gene is located downstream of the *bscI* gene (Fig. 1A), and the BscJ protein is
321 predicted to function as an inner membrane ring (SctJ), a component of the T3SS. The
322 signal intensity of BscJ was not decreased in the WCL sample of the BspR/Bcr4
323 double-deficient strain (Δ*bspR*Δ*bcr4*) compared to that of Δ*bspR* (Fig. 6A), suggesting that

bioRxiv preprint doi: https://doi.org/10.1101/2021.09.28.462275; this version posted August 9, 2022. The copyright holder for this preprint (which was not certified by peer review) is the author/funder, who has granted bioRxiv a license to display the preprint in perpetuity. It is made available under aCC-BY 4.0 International license.

324 Bcr4 is not involved in the stability of BscJ. Therefore, it is suggested that Bcr4 specifically
325 stabilizes BscI. In order to detect the interaction between Bcr4 and BscI in the *B.*
326 *bronchiseptica* cells, immunoprecipitation was performed using anti-BscI antibody against
327 Δ*bspR* lysate. The immunoprecipitated fractions were analyzed by Western blotting using
328 anti-BscI antibody; however, an evident BscI signal was not detected (data not shown). The
329 results of our immunoprecipitation assay were thus unable to demonstrate a specific
330 interaction between Bcr4 and BscI. We speculate that *B. bronchiseptica* did not maintain
331 a sufficient amount of BscI in whole cell lysate to detect the interaction by
332 immunoprecipitation. In Fig. 6B, we obtained an extra signal around 33 kDa in Western
333 blotting using anti-Bcr4 antibody when we analyzed the lysate of *B. bronchiseptica* treated
334 with a cross-linker, DSS. When we performed the Western blotting using anti-BscI antibody
335 for the cross-linked lysate, the extra signal was not detected (data not shown).
336 In order to examine whether Bcr4 has structural similarity to any chaperones for the type
337 III secreted proteins produced by other bacteria, we used AlphaFold2. As a result, we
338 detected significant structural similarities to the other chaperones, *Aeromonas* AcrH (34)
339 and *Pseudomonas* PscG (35) (Fig. S7). Although we obtained no plausible structural model
340 for the interaction between BscI and Bcr4, the results strongly suggest that Bcr4 is a
341 chaperone.
342 It is still unclear how Bcr4 antagonizes the BspR-negative regulation activity, and how
343 overexpression of Bcr4 promotes the production and secretion of type III secreted proteins

bioRxiv preprint doi: https://doi.org/10.1101/2021.09.28.462275; this version posted August 9, 2022. The copyright holder for this preprint (which was not certified by peer review) is the author/funder, who has granted bioRxiv a license to display the preprint in perpetuity. It is made available under aCC-BY 4.0 International license.

344 in *B. bronchiseptica*. Further analysis is needed to elucidate the detailed molecular
345 mechanism by which Bcr4 contributes to the regulation and establishment of the T3SS.
346
347
348
349
350
351
352
353
354
355
356
357
358
359

bioRxiv preprint doi: https://doi.org/10.1101/2021.09.28.462275; this version posted August 9, 2022. The copyright holder for this preprint (which was not certified by peer review) is the author/funder, who has granted bioRxiv a license to display the preprint in perpetuity. It is made available under aCC-BY 4.0 International license.

360 **Materials and Methods**

361 **Bacterial strains and cell culture.**

362 The strains used in this study are listed in Table 1. *B. bronchiceptica* S798 (6) was used
363 as the wild-type strain. Δ*bscN* (a BscN-deficient strain), Δ*bcr4* (a Bcr4-deficient strain),
364 Δ*bspR* (a BspR-deficient strain) and Δ*bspR*Δ*bcr4* (a BspR and Bcr4-deficient strain) have
365 been described elsewhere (6, 14, 24). *Escherichia coli* DH10B, BL21 (36) and Sm10λ*pir*
366 were used for DNA cloning, recombinant protein expression and conjugation, respectively
367 (Table 1). *B. bronchiceptica* was grown on Bordet-Gengou agar plates at 37ºC for 2 days.
368 Fresh colonies of *B. bronchiceptica* were cultured in Stainer-Scholt (SS) medium (37) with a
369 starting A_{600} of 0.23 under vigorous shaking conditions at 37ºC. L2 cells, a rat lung epithelial
370 cell line (ATCC CCL-149), were maintained in F-12K (Invitrogen). The cell culture medium
371 was supplemented with 10% fetal calf serum (FCS). L2 cells were grown at 37°C under a
372 5% CO_2 atmosphere.

373

374 **Preparation of proteins from culture supernatants and whole bacterial cell lysates.**

375 Proteins secreted into bacterial culture supernatants and whole bacterial cell lysates
376 were prepared as described previously (38). The loaded sample amounts were adjusted by
377 the A_{600} of each bacterial culture to load samples prepared from the same amounts of
378 bacteria. The protein samples were separated by SDS-PAGE and analyzed by Western
379 blotting.

bioRxiv preprint doi: https://doi.org/10.1101/2021.09.28.462275; this version posted August 9, 2022. The copyright holder for this preprint (which was not certified by peer review) is the author/funder, who has granted bioRxiv a license to display the preprint in perpetuity. It is made available under aCC-BY 4.0 International license.

380

381 **Antibodies.**

382 Anti-BteA, anti-BopD, anti-Bsp22, BspR, BopB, and anti-Bcr4 antibodies were purified
383 from rabbit serum in our previous study (6, 7, 10, 14, 24, 39). Mouse anti-V5 and anti-RNA
384 polymerase beta subunit (RpoB) monoclonal antibodies were purchased from Santa Cruz
385 Biotechnology and BioLegend, respectively. To detect filamentous hemagglutinin (FHA)
386 signals, we used mouse anti-FHA serum kindly gifted from K. Kamachi (National Institute of
387 Infectious Diseases). To prepare the anti-BscI and anti-BscJ antibodies, the peptides
388 corresponding to the C-terminus regions of BscI (CKAIGRATQNVDTLARMS) and BscJ
389 (CRGEGRGGAGAGATEGAGHD) were conjugated with hemocyanin from keyhole limpets
390 (Sigma), respectively, by using 3-maleimidobenzoic acid N-hydroxysuccinimide ester
391 (Sigma). These cross-linked peptides were used to immunize rabbits, and the resulting
392 anti-sera were incubated with the same peptides immobilized on epoxy-activated
393 sepharose 6B (Amersham) to obtain specific Ig-fractions.

394

395 **Immunofluorescence staining of L2 cells infected with *B. bronchiseptica.***

396 Immunofluorescent staining assay was performed as previously described (38), with
397 slight modifications. Briefly, L2 cells were seeded on coverslips in 6-well plates and
398 incubated overnight. In order to detect adequate amounts of Bsp22 signals, we infected the
399 L2 cells with *B. bronchiseptica* cultured in iron-depleted SS medium at an MOI of 2000. To

bioRxiv preprint doi: https://doi.org/10.1101/2021.09.28.462275; this version posted August 9, 2022. The copyright holder for this preprint (which was not certified by peer review) is the author/funder, who has granted bioRxiv a license to display the preprint in perpetuity. It is made available under aCC-BY 4.0 International license.

400 avoid excessive killing of L2 cells with bacteria, the plates were not centrifuged. After being
401 incubated for 1 h at 37°C under a 5% CO_2 atmosphere, the infected L2 cells were
402 immunostained. Average numbers of Bsp22 signals on single L2 cells were measured by a
403 fluorescence microscope.
404
405 **LDH Assays.**
406 LDH assays were performed as previously described (38). Briefly, to examine whether
407 lactate dehydrogenase (LDH) is released from *B. bronchiseptica*-infected cells, $5.0×10^4$
408 cells/well of L2 cells seeded in 24-well plates were infected with bacteria at an MOI of 50 or
409 200. The plates were centrifuged at 900×*g* for 5 min and incubated for 3 h at 37ºC under a
410 5% CO_2 atmosphere. The amounts of LDH were measured spectrophotometrically using a
411 Cyto-Tox 96 Non-radioactive Cytotoxicity Assay kit (Promega). The LDH (%) level is shown
412 as a ratio, with the value obtained from the well treated with 0.1% Triton X-100 set as
413 100%.
414
415 **Cross-linking Assay**
416 The cross-linking assay was performed as previously described (40). A 100 μL culture of
417 *B. bronchiseptica* was centrifuged at 20,000×*g* and the supernatant was removed. The
418 pellet was washed with PBS and resuspended in 100 μL of PBS. Then, disuccinimidyl
419 suberate (DSS (Thermo)) dissolved in DMSO was added at a final concentration of 10 mM.

bioRxiv preprint doi: https://doi.org/10.1101/2021.09.28.462275; this version posted August 9, 2022. The copyright holder for this preprint (which was not certified by peer review) is the author/funder, who has granted bioRxiv a license to display the preprint in perpetuity. It is made available under aCC-BY 4.0 International license.

420 After incubation on ice for 1 h, Tris-HCl pH8.0 was added at a final concentration of 50 mM.
421 The solution was centrifuged at 20,000×*g*, and the supernatant was removed. The pellet
422 was dissolved in 2×SDS-PAGE sample buffer. The samples were prepared from the same
423 amounts of bacteria based on the A_{600} values of the bacterial culture, then separated by
424 SDS-PAGE, and analyzed by Western blotting.
425
426 **Statistical analyses**
427 The statistical analyses were performed using the nonparametric test with a two-tailed
428 p-value with Prism ver. 5.0f software (Graphpad, La Jolla, CA). Values of $p<0.05$ were
429 considered significant.
430
431 **Others**
432 The pull-down assay, the construction of *bscI* gene-disrupted or *bspR*/*bscI* double strains,
433 the construction of the plasmids used for producing Bcr4 derivatives and BscI
434 complementation, the quantitative reverse transcription-PCR, and Protein structure
435 prediction are described in Text S. Plasmids and Primers used in this study are listed in
436 Table S2 and S3, respectively.
437
438
439

bioRxiv preprint doi: https://doi.org/10.1101/2021.09.28.462275; this version posted August 9, 2022. The copyright holder for this preprint (which was not certified by peer review) is the author/funder, who has granted bioRxiv a license to display the preprint in perpetuity. It is made available under aCC-BY 4.0 International license.

440

441

bioRxiv preprint doi: https://doi.org/10.1101/2021.09.28.462275; this version posted August 9, 2022. The copyright holder for this preprint (which was not certified by peer review) is the author/funder, who has granted bioRxiv a license to display the preprint in perpetuity. It is made available under aCC-BY 4.0 International license.

442 **Acknowledgements**

443 This work was supported in part by grants (19K07542 to A.A.; 20K07485 to A.K.;
444 19K07561 to T.H.) from the Ministry of Education, Culture, Sports, Science and Technology
445 and the Japan Society for the Promotion of Science (KAKENHI), and a grant
446 (JP22gm1610003 to M.S. and A.K.) from the Japan Agency for Medical Research and
447 Development (AMED).
448 The funders had no role in the study design, date collection or analysis, the decision to
449 publish, or the preparation of manuscript.
450
451
452
453
454
455
456
457
458
459
460
461

bioRxiv preprint doi: https://doi.org/10.1101/2021.09.28.462275; this version posted August 9, 2022. The copyright holder for this preprint (which was not certified by peer review) is the author/funder, who has granted bioRxiv a license to display the preprint in perpetuity. It is made available under aCC-BY 4.0 International license.

462 **References**

463 1. Goodnow RA. 1980. Biology of *Bordetella bronchiseptica*. Microbiol Rev 44:722-38.

464 2. Mattoo S, Cherry JD. 2005. Molecular pathogenesis, epidemiology, and clinical
465 manifestations of respiratory infections due to *Bordetella pertussis* and other
466 *Bordetella* subspecies. Clin Microbiol Rev 18:326-82.

467 3. Cornelis GR, Van Gijsegem F. 2000. Assembly and function of type III secretory
468 systems. Annu Rev Microbiol 54:735-74.

469 4. Büttner D. 2012. Protein export according to schedule: architecture, assembly, and
470 regulation of type III secretion systems from plant- and animal-pathogenic bacteria.
471 Microbiol Mol Biol Rev 76:262-310.

472 5. Deng W, Marshall NC, Rowland JL, McCoy JM, Worrall LJ, Santos AS, Strynadka
473 NCJ, Finlay BB. 2017. Assembly, structure, function and regulation of type III
474 secretion systems. Nat Rev Microbiol 15:323-337.

475 6. Kuwae A, Ohishi M, Watanabe M, Nagai M, Abe A. 2003. BopB is a type III secreted
476 protein in *Bordetella bronchiseptica* and is required for cytotoxicity against cultured
477 mammalian cells. Cell Microbiol 5:973-83.

478 7. Nogawa H, Kuwae A, Matsuzawa T, Abe A. 2004. The type III secreted protein BopD
479 in *Bordetella bronchiseptica* is complexed with BopB for pore formation on the host
480 plasma membrane. J Bacteriol 186:3806-13.

481 8. Yuk MH, Harvill ET, Cotter PA, Miller JF. 2000. Modulation of host immune

bioRxiv preprint doi: https://doi.org/10.1101/2021.09.28.462275; this version posted August 9, 2022. The copyright holder for this preprint (which was not certified by peer review) is the author/funder, who has granted bioRxiv a license to display the preprint in perpetuity. It is made available under aCC-BY 4.0 International license.

482 responses, induction of apoptosis and inhibition of NF-kappaB activation by the
483 *Bordetella* type III secretion system. Mol Microbiol 35:991-1004.
484 9. Panina EM, Mattoo S, Griffith N, Kozak NA, Yuk MH, Miller JF. 2005. A genome-wide
485 screen identifies a Bordetella type III secretion effector and candidate effectors in
486 other species. Mol Microbiol 58:267-79.
487 10. Kuwae A, Matsuzawa T, Ishikawa N, Abe H, Nonaka T, Fukuda H, Imajoh-Ohmi S,
488 Abe A. 2006. BopC is a novel type III effector secreted by *Bordetella bronchiseptica*
489 and has a critical role in type III-dependent necrotic cell death. J Biol Chem
490 281:6589-600.
491 11. Nagamatsu K, Kuwae A, Konaka T, Nagai S, Yoshida S, Eguchi M, Watanabe M,
492 Mimuro H, Koyasu S, Abe A. 2009. *Bordetella* evades the host immune system by
493 inducing IL-10 through a type III effector, BopN. J Exp Med 206:3073-88.
494 12. Abe A, Nishimura R, Kuwae A. 2017. *Bordetella* effector BopN is translocated into
495 host cells via its N-terminal residues. Microbiol Immunol 61:206-214.
496 13. Ahuja U, Liu M, Tomida S, Park J, Souda P, Whitelegge J, Li H, Harvill ET, Parkhill J,
497 Miller JF. 2012. Phenotypic and genomic analysis of hypervirulent human-associated
498 *Bordetella bronchiseptica*. BMC Microbiol 12:167.
499 14. Kurushima J, Kuwae A, Abe A. 2012. The type III secreted protein BspR regulates
500 the virulence genes in *Bordetella bronchiseptica*. PLoS One 7:e38925.
501 15. Medhekar B, Shrivastava R, Mattoo S, Gingery M, Miller JF. 2009. *Bordetella* Bsp22

bioRxiv preprint doi: https://doi.org/10.1101/2021.09.28.462275; this version posted August 9, 2022. The copyright holder for this preprint (which was not certified by peer review) is the author/funder, who has granted bioRxiv a license to display the preprint in perpetuity. It is made available under aCC-BY 4.0 International license.

502 forms a filamentous type III secretion system tip complex and is immunoprotective in
503 vitro and in vivo. Mol Microbiol 71:492-504.
504 16. Ahuja U, Shokeen B, Cheng N, Cho Y, Blum C, Coppola G, Miller JF. 2016.
505 Differential regulation of type III secretion and virulence genes in *Bordetella*
506 *pertussis* and *Bordetella bronchiseptica* by a secreted anti-sigma factor. Proc Natl
507 Acad Sci U S A 113:2341-8.
508 17. Feldman MF, Cornelis GR. 2003. The multitalented type III chaperones: all you can
509 do with 15 kDa. FEMS Microbiol Lett 219:151-8.
510 18. Stebbins CE, Galán JE. 2001. Maintenance of an unfolded polypeptide by a cognate
511 chaperone in bacterial type III secretion. Nature 414:77-81.
512 19. Lloyd SA, Norman M, Rosqvist R, Wolf-Watz H. 2001. *Yersinia* YopE is targeted for
513 type III secretion by N-terminal, not mRNA, signals. Mol Microbiol 39:520-31.
514 20. Lee SH, Galán JE. 2004. *Salmonella* type III secretion-associated chaperones
515 confer secretion-pathway specificity. Mol Microbiol 51:483-95.
516 21. Quinaud M, Chabert J, Faudry E, Neumann E, Lemaire D, Pastor A, Elsen S,
517 Dessen A, Attree I. 2005. The PscE-PscF-PscG complex controls type III secretion
518 needle biogenesis in *Pseudomonas aeruginosa*. J Biol Chem 280:36293-300.
519 22. Wood SE, Jin J, Lloyd SA. 2008. YscP and YscU switch the substrate specificity of
520 the *Yersinia* type III secretion system by regulating export of the inner rod protein
521 YscI. J Bacteriol 190:4252-62.

bioRxiv preprint doi: https://doi.org/10.1101/2021.09.28.462275; this version posted August 9, 2022. The copyright holder for this preprint (which was not certified by peer review) is the author/funder, who has granted bioRxiv a license to display the preprint in perpetuity. It is made available under aCC-BY 4.0 International license.

522 23. Monlezun L, Liebl D, Fenel D, Grandjean T, Berry A, Schoehn G, Dessein R, Faudry
523 E, Attree I. 2015. PscI is a type III secretion needle anchoring protein with in vitro
524 polymerization capacities. Mol Microbiol 96:419-36.
525 24. Nishimura R, Abe A, Sakuma Y, Kuwae A. 2018. *Bordetella bronchiseptica* Bcr4
526 antagonizes the negative regulatory function of BspR via its role in type III secretion.
527 Microbiol Immunol 62:743-754.
528 25. Wattiau P, Bernier B, Deslée P, Michiels T, Cornelis GR. 1994. Individual chaperones
529 required for Yop secretion by *Yersinia*. Proc Natl Acad Sci U S A 91:10493-7.
530 26. Kamanova J. 2020. *Bordetella* Type III Secretion Injectosome and Effector Proteins.
531 Front Cell Infect Microbiol 10:466.
532 27. Yuk MH, Harvill ET, Miller JF. 1998. The BvgAS virulence control system regulates
533 type III secretion in *Bordetella bronchiseptica*. Mol Microbiol 28:945-59.
534 28. Kurushima J, Kuwae A, Abe A. 2012. Iron starvation regulates the type III secretion
535 system in *Bordetella bronchiseptica*. Microbiol Immunol 56:356-62.
536 29. Sun P, Tropea JE, Austin BP, Cherry S, Waugh DS. 2008. Structural characterization
537 of the *Yersinia pestis* type III secretion system needle protein YscF in complex with
538 its heterodimeric chaperone YscE/YscG. J Mol Biol 377:819-30.
539 30. Day JB, Guller I, Plano GV. 2000. *Yersinia pestis* YscG protein is a Syc-like
540 chaperone that directly binds yscE. Infect Immun 68:6466-71.
541 31. Francis MS, Aili M, Wiklund ML, Wolf-Watz H. 2000. A study of the YopD-lcrH

bioRxiv preprint doi: https://doi.org/10.1101/2021.09.28.462275; this version posted August 9, 2022. The copyright holder for this preprint (which was not certified by peer review) is the author/funder, who has granted bioRxiv a license to display the preprint in perpetuity. It is made available under aCC-BY 4.0 International license.

542 interaction from *Yersinia pseudotuberculosis* reveals a role for hydrophobic residues
543 within the amphipathic domain of YopD. Mol Microbiol 38:85-102.
544 32. Woestyn S, Sory MP, Boland A, Lequenne O, Cornelis GR. 1996. The cytosolic SycE
545 and SycH chaperones of *Yersinia* protect the region of YopE and YopH involved in
546 translocation across eukaryotic cell membranes. Mol Microbiol 20:1261-71.
547 33. Yang H, Shan Z, Kim J, Wu W, Lian W, Zeng L, Xing L, Jin S. 2007. Regulatory role
548 of PopN and its interacting partners in type III secretion of *Pseudomonas aeruginosa*.
549 J Bacteriol 189:2599-609.
550 34. Nguyen VS, Jobichen C, Tan KW, Tan YW, Chan SL, Ramesh K, Yuan Y, Hong Y,
551 Seetharaman J, Leung KY, Sivaraman J, Mok YK. 2015. Structure of AcrH-AopB
552 Chaperone-Translocator Complex Reveals a Role for Membrane Hairpins in Type III
553 Secretion System Translocon Assembly. Structure 23:2022-31.
554 35. Quinaud M, Ple S, Job V, Contreras-Martel C, Simorre JP, Attree I, Dessen A. 2007.
555 Structure of the heterotrimeric complex that regulates type III secretion needle
556 formation. Proc Natl Acad Sci U S A 104:7803-8.
557 36. Studier FW, Moffatt BA. 1986. Use of bacteriophage T7 RNA polymerase to direct
558 selective high-level expression of cloned genes. J Mol Biol 189:113-30.
559 37. Stainer DW, Scholte MJ. 1970. A simple chemically defined medium for the
560 production of phase I *Bordetella pertussis*. J Gen Microbiol 63:211-20.
561 38. Goto M, Hanawa T, Abe A, Kuwae A. 2020. Transcriptional Downregulation of a Type

bioRxiv preprint doi: https://doi.org/10.1101/2021.09.28.462275; this version posted August 9, 2022. The copyright holder for this preprint (which was not certified by peer review) is the author/funder, who has granted bioRxiv a license to display the preprint in perpetuity. It is made available under aCC-BY 4.0 International license.

562 III Secretion System under Reducing Conditions in *Bordetella pertussis*. J Bacteriol
563 202.
564 39. Kurushima J, Kuwae A, Abe A. 2012. Btc22 chaperone is required for secretion and
565 stability of the type III secreted protein Bsp22 in *Bordetella bronchiseptica*. FEMS
566 Microbiol Lett 331:144-51.
567 40. Rappl C, Deiwick J, Hensel M. 2003. Acidic pH is required for the functional
568 assembly of the type III secretion system encoded by *Salmonella* pathogenicity
569 island 2. FEMS Microbiol Lett 226:363-72.
570
571
572
573
574
575
576
577
578
579
580
581

bioRxiv preprint doi: https://doi.org/10.1101/2021.09.28.462275; this version posted August 9, 2022. The copyright holder for this preprint (which was not certified by peer review) is the author/funder, who has granted bioRxiv a license to display the preprint in perpetuity. It is made available under aCC-BY 4.0 International license.

582 **Figure legends**

583 **Fig. 1. The interaction of Bcr4 with inner rod protein BscI.** (A) The *bcr4* gene and its
584 peripheral genes localized in the T3SS apparatus locus (*bsc* locus) on the *B.*
585 *bronchiseptica* S798 chromosome are depicted. (B) The purified Bcr4 (Bcr4-Strep) was
586 loaded on Strep-Tactin beads. Then, the Bcr4-Strep-loaded beads (Bcr4) and the beads
587 alone (beads) were mixed with the lysates prepared from *E. coli* BL21 producing BscI,
588 BscK or BscJ tagged with V5 (BscI-V5, BscK-V5 or BscJ-V5), respectively. After 3 h
589 incubation at 4□, each supernatant was prepared as the supernatant fraction (Sup) sample,
590 and each pellet was washed with TBS or TBS containing 0.1% Triton X-100 (Triton) and
591 prepared as the pellet fraction (Pellet) sample. The Sup and Pellet samples were separated
592 by SDS-PAGE and analyzed by Western blotting (WB) with anti-V5 antibody (top). Pellet
593 samples were also stained with Coomassie Brilliant Blue (CBB, bottom). (C) The purified
594 BscI (BscI-Strep) or N-terminal moiety of BteA (amino acids region 1–312, BteA-N-Strep)
595 were loaded on Strep-Tactin beads. Then, the beads were mixed with the lysate prepared
596 from *E. coli* BL21 to produce Bcr4 tagged with V5 (Bcr4-V5) at 4□ for 3 h. The prepared
597 Sup and Pellet samples were separated by SDS-PAGE and analyzed by WB with anti-V5
598 antibody (top). Pellet samples were also stained with CBB (bottom). Experiments were
599 performed at least three times, and representative data are shown.

600

601 **Fig. 2. Pull-down assays between BscI and truncated versions of Bcr4.** (A) Bcr4

bioRxiv preprint doi: https://doi.org/10.1101/2021.09.28.462275; this version posted August 9, 2022. The copyright holder for this preprint (which was not certified by peer review) is the author/funder, who has granted bioRxiv a license to display the preprint in perpetuity. It is made available under aCC-BY 4.0 International license.

602 derivatives used for pull-down assay are depicted. (B) The purified Bcr4-FL, Bcr4Δ58-109
603 or Bcr4Δ110-173 (Bcr4-FL-Strep, Bcr4Δ58-109-Strep or Bcr4Δ110-17-Strep) was loaded on
604 Strep-Tactin beads, and then the beads were mixed with the lysate prepared from *E. coli*
605 BL21, producing BscI-V5, respectively. After 3 h incubation at 4□, the supernatant fraction
606 (Sup) and pellet fraction (Pellet) samples were prepared. The Sup and Pellet samples were
607 separated by SDS-PAGE and analyzed by Western blotting (WB) with anti-V5 antibody
608 (top), and stained with Coomassie Brilliant Blue (CBB, bottom). Experiments were
609 performed at least three times, and representative data are shown.
610
611 **Fig. 3. The Bcr4 domain required for T3SS activity** (A) Bcr4 derivatives used for the
612 analysis of T3SS activity are depicted. (B) The *B. bronchiseptica* wild-type strain,
613 Bcr4-deficient strain (Δ*bcr4*), and Δ*bcr4* producing Bcr4-FL-FLAG (Δ*bcr4*+*bcr4*-FL-FLAG),
614 Bcr4Δ169-173-FLAG (Δ*bcr4*+*bcr4*Δ169-173-FLAG), Bcr4Δ164-173-FLAG (Δ*bcr4*+*bcr4*
615 Δ164-173-FLAG), and Bcr4Δ159-173-FLAG (Δ*bcr4*+*bcr4*Δ159-173-FLAG) were cultured in
616 SS medium. Whole cell lysates (WCL) and culture supernatant fraction (CS) samples were
617 separated by SDS-PAGE and analyzed by Western blotting using antibodies against Bcr4,
618 FLAG, BteA, BopD or RpoB. RpoB was used as an internal loading control. AP indicates
619 the amino acids region of the antigen peptide used for anti-Bcr4 antibody generation. WCL
620 and CS samples were prepared from equal volumes of bacterial culture. When we
621 performed Western blotting using anti-BteA or BopD antibodies, we loaded a 100- or

bioRxiv preprint doi: https://doi.org/10.1101/2021.09.28.462275; this version posted August 9, 2022. The copyright holder for this preprint (which was not certified by peer review) is the author/funder, who has granted bioRxiv a license to display the preprint in perpetuity. It is made available under aCC-BY 4.0 International license.

622 50-fold smaller amount of Δ*bcr4*+*bcr4*-FL-FLAG, Δ*bcr4*+*bcr4*Δ169-173-FLAG and
623 Δ*bcr4*+*bcr4*Δ164-173-FLAG CS samples on the SDS-PAGE gel than on the wild-type,
624 Δ*bcr4* and Δ*bcr4*+*bcr4*Δ159-173-FLAG CS samples to avoid obtaining excess signal
625 intensities. The numbers at the bottom of the lower panel indicate the relative signal
626 intensity of RpoB measured using ImageJ software. (C) L2 cells were infected with each
627 strain at an moi of 50 for 1 h. The amounts of LDH released into the extracellular medium
628 from infected cells are shown, and the relative cytotoxicity (percent) was determined as
629 described in the Materials and Methods. Error bars indicate the SEMs from triplicate
630 experiments. *P<0.05. Experiments were performed at least three times, and
631 representative data are shown.

632

633 **Fig. 4. The effect of BscI deletion on T3SS activity in *B. bronchiseptica*.** (A) Whole cell
634 lysates (WCL) and culture supernatant fraction (CS) samples were prepared from the
635 wild-type strain, Δ*bscI* (BscI-deficient strain), Δ*bscI*+*bscI* (BscI-complemented strain) and
636 Δ*bscN* (T3SS-inactive strain) cultured in SS medium. WCL and CS samples were
637 separated by SDS-PAGE and analyzed by Western blotting using antibodies against BscI,
638 BteA, BopD, Bsp22, FHA or RpoB. BscI tagged with Strep (BscI-Strep) was loaded as a
639 control. *BscI-Strep signal; **NS (nonspecific signals); ***A faint signal of BscI. The
640 numbers at the bottom of the lower panel indicate the relative signal intensity of RpoB
641 measured using ImageJ software. (B) WCL and CS were prepared from the wild-type,

bioRxiv preprint doi: https://doi.org/10.1101/2021.09.28.462275; this version posted August 9, 2022. The copyright holder for this preprint (which was not certified by peer review) is the author/funder, who has granted bioRxiv a license to display the preprint in perpetuity. It is made available under aCC-BY 4.0 International license.

642 Δ*bspR* (BspR-deficient strain), Δ*bspR*Δ*bscI* (BspR- and BscI-deficient strain) and
643 Δ*bspR*Δ*bscI*+*bscI* (BscI-complemented BspR- and Bcr4-deficient strain) cultured in SS
644 medium. WCL and CS were separated by SDS-PAGE and analyzed by Western blotting
645 using antibodies against BscI, BspR, Bsp22 or BopB antibodies. Loaded WCL and CS
646 samples were prepared from equal volumes of bacterial culture. When we performed
647 Western blotting using antibodies against Bsp22 or BopB, we loaded a 25- or 5-fold smaller
648 amount of Δ*bspR*, Δ*bspR*Δ*bscI* and Δ*bspR*Δ*bscI*+*bscI* WCL samples, and 5- or 10-fold
649 smaller amount of Δ*bspR* and Δ*bspR*Δ*bscI*+*bscI* CS samples on the SDS-PAGE gel than
650 the wild-type to avoid obtaining excess signal intensities. Experiments were performed at
651 least three times, and representative data are shown.
652

653 **Fig. 5. Immunofluorescent staining of Bsp22 on L2 cells infected with *B.***
654 ***bronchiseptica* and the results of the LDH assay.** (A) L2 cells were infected with the
655 wild-type strain, Δ*bscI* (BscI-deficient strain), Δ*bscI*+*bscI* (BscI-complemented strain) or
656 Δ*bscN* (T3SS-inactive strain) as described in the Materials and Methods. After fixation, cells
657 were stained with anti-Bsp22 antibody (green), rhodamine phalloidin (red) and DAPI (blue).
658 The inset shows higher magnification of the boxed area in the image. Arrowheads and
659 arrows indicate the signals of Bsp22 (green) and bacteria, respectively. (B) Bsp22 signals
660 per one cell were counted under a fluorescent microscope. At least 120 cells were
661 randomly chosen. (C) The results of LDH assay at an MOI of 200 are shown as a histogram.

bioRxiv preprint doi: https://doi.org/10.1101/2021.09.28.462275; this version posted August 9, 2022. The copyright holder for this preprint (which was not certified by peer review) is the author/funder, who has granted bioRxiv a license to display the preprint in perpetuity. It is made available under aCC-BY 4.0 International license.

662 Error bars indicate the SEMs from triplicate experiments. *P<0.05. Experiments were
663 performed at least three times, and representative data are shown.
664
665 **Fig. 6. The effect of Bcr4 on BscI stability and the suggestive interaction of Bcr4 with**
666 **BscI in *B. bronchiseptica*.** (A) The whole cell lysates (WCL) and culture supernatant
667 fraction (CS) were prepared from the wild-type strain, Δ*bcr4* (Bcr4-deficient strain), Δ*bspR*
668 (BspR-deficient strain) or Δ*bspR*Δ*bcr4* (BspR- and Bcr4-deficient strain) cultured in SS
669 medium. WCL and CS were separated by SDS-PAGE and analyzed by Western blotting
670 with antibodies against BscI (inner-rod protein), BscJ (inner-ring protein) and Bcr4. The
671 samples were prepared from equal volumes of bacterial culture. When we carried out
672 Western blotting using anti-BscJ or Bcr4 antibodies, we loaded a 10-fold-smaller amount of
673 Δ*bspR* or Δ*bspR*Δ*bcr4* WCL samples on the SDS-PAGE than WT or Δ*bcr4* WCL samples to
674 avoid obtaining excess signal intensities. (B) WCL were prepared from the wild-type, Δ*bspR*
675 or Δ*bspR*Δ*bcr4* treated with (+) or without (−) cross linker disuccinimidyl suberate (DSS).
676 WCL were separated by SDS-PAGE and analyzed by Western blotting with anti-Bcr4
677 antibody. The lower panel is a short exposure of the upper panel. Experiments were
678 performed at least three times, and representative data are shown.
679
680 **Fig. 7. Schematic depiction of the Bcr4 and BscI functions.** In the *B. bronchiseptica*
681 bacterial cytosol, Bcr4 (blue) stabilizes BscI (orange). Then, BscI is presumed to be

bioRxiv preprint doi: https://doi.org/10.1101/2021.09.28.462275; this version posted August 9, 2022. The copyright holder for this preprint (which was not certified by peer review) is the author/funder, who has granted bioRxiv a license to display the preprint in perpetuity. It is made available under aCC-BY 4.0 International license.

682 localized to the T3SS machinery (gray) and form the inner rod. BscI is essential for T3SS
683 activity and secreted from the bacterial cell. BscJ (pink) is predicted to function as an inner
684 membrane ring. Bsp22 (green) forms a filament-like structure. OM and IM indicate the outer
685 membrane (white) and inner membrane (white), respectively.
686
687
688
689
690
691
692
693
694
695
696
697
698
699
700
701

bioRxiv preprint doi: https://doi.org/10.1101/2021.09.28.462275; this version posted August 9, 2022. The copyright holder for this preprint (which was not certified by peer review) is the author/funder, who has granted bioRxiv a license to display the preprint in perpetuity. It is made available under aCC-BY 4.0 International license.

Table 1. Bacterial strains used in the study

Name	Relevant genotype	Reference or source
B. bronchiseptica		
S798	wild-type strain	6
Δ*bscI*	BscI-deficient strain	This study
Δ*bscN*	BscN-deficient strain	6
Δ*bcr4*	Bcr4-deficient strain	24
Δ*bspR*	BspR-deficient strain	14
Δ*bspR*Δ*bscI*	BspR and BscI-deficient strain	This study
Δ*bspR*Δ*bcr4*	BspR- and Bcr4-deficient strain	24
E. coli		
DH10B	Host strain for pDONR201, p99-*ccdB*-V5 and pRK415-R4-R3-F	Invitrogen
BL21	Host strain for pColdII	36
Sm10λ*pir*	Host strain for pABB-CRS2	6

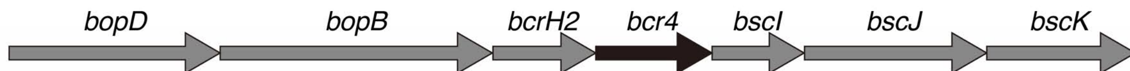

bioRxiv preprint doi: https://doi.org/10.1101/2021.09.28.462275; this version posted August 9, 2022. The copyright holder for this preprint (which was not certified by peer review) is the author/funder, who has granted bioRxiv a license to display the preprint in perpetuity. It is made available under aCC-BY 4.0 International license.

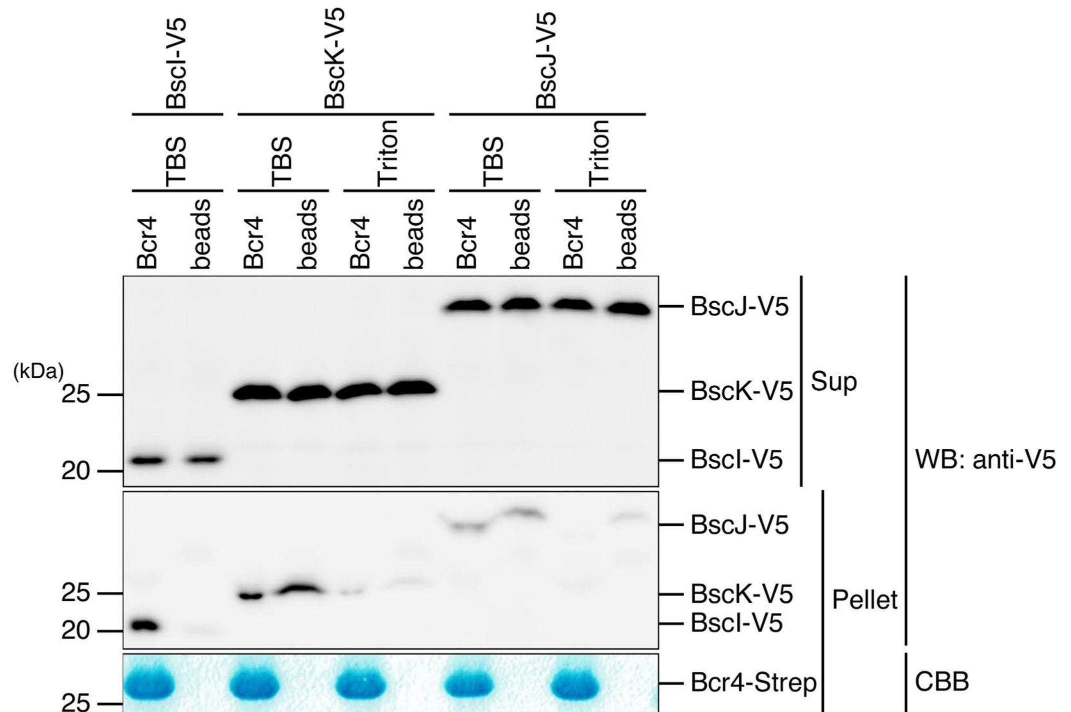

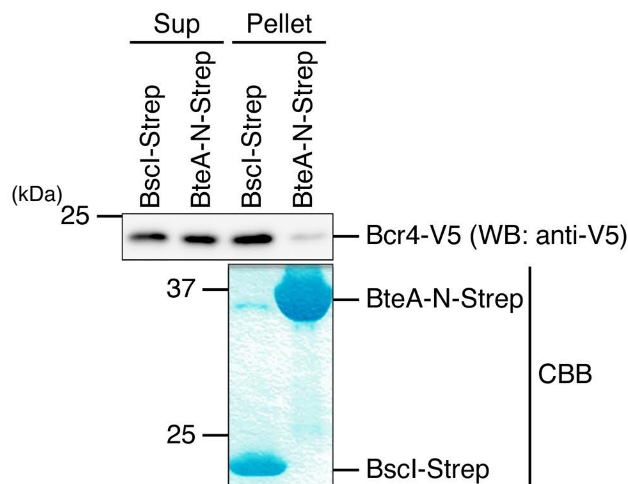

Fig. 1. The interaction of Bcr4 with inner rod protein BscI. (A) The *bcr4* gene and its peripheral genes localized in the T3SS apparatus locus (*bsc* locus) on the *B. bronchiseptica* S798 chromosome are depicted. (B) The purified Bcr4 (Bcr4-Strep) was loaded on Strep-Tactin beads. Then, the Bcr4-Strep-loaded beads (Bcr4) and the beads alone (beads) were mixed with the lysates prepared from *E. coli* BL21 producing BscI, BscK or BscJ tagged with V5 (BscI-V5, BscK-V5 or BscJ-V5), respectively. After 3 h incubation at 4°C, each supernatant was prepared as the supernatant fraction (Sup) sample, and each pellet was washed with TBS or TBS containing 0.1% Triton X-100 (Triton) and prepared as the pellet fraction (Pellet) sample. The Sup and Pellet samples were separated by SDS-PAGE and analyzed by Western blotting (WB) with anti-V5 antibody (top). Pellet samples were also stained with Coomassie Brilliant Blue (CBB, bottom). (C) The purified BscI (BscI-Strep) or N-terminal moiety of BteA (amino acids region 1–312, BteA-N-Strep) were loaded on Strep-Tactin beads. Then, the beads were mixed with the lysate prepared from *E. coli* BL21 to produce Bcr4 tagged with V5 (Bcr4-V5) at 4°C for 3 h. The prepared Sup and Pellet samples were separated by SDS-PAGE and analyzed by WB with anti-V5 antibody (top). Pellet samples were also stained with CBB (bottom). Experiments were performed at least three times, and representative data are shown.

Fig. 1

bioRxiv preprint doi: https://doi.org/10.1101/2021.09.28.462275; this version posted August 9, 2022. The copyright holder for this preprint (which was not certified by peer review) is the author/funder, who has granted bioRxiv a license to display the preprint in perpetuity. It is made available under aCC-BY 4.0 International license.

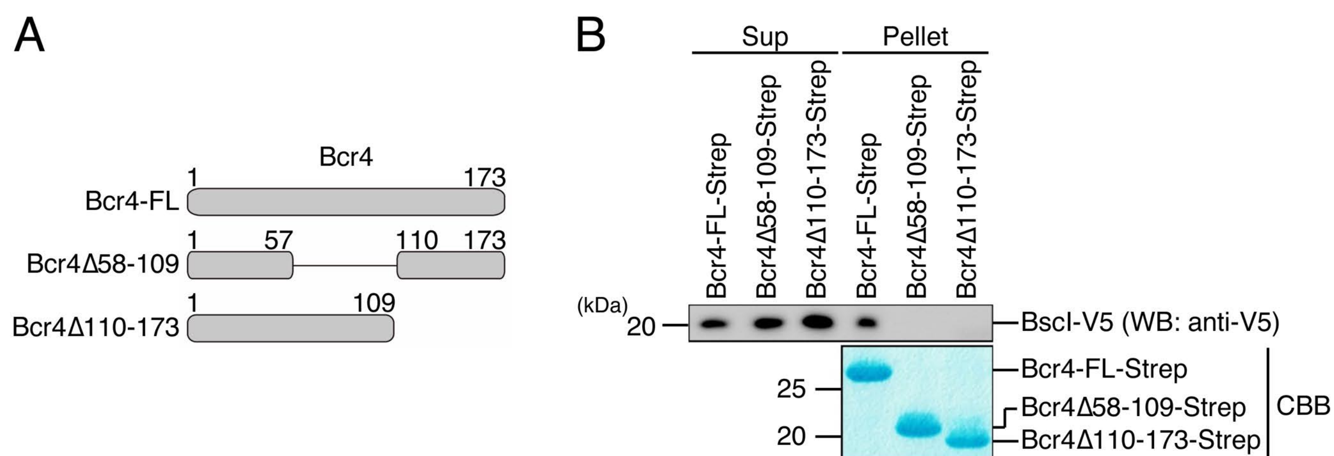

Fig. 2. Pull-down assays between BscI and truncated versions of Bcr4. (A) Bcr4 derivatives used for pull-down assay are depicted. (B) The purified Bcr4-FL, Bcr4Δ58-109 or Bcr4Δ110-173 (Bcr4-FL-Strep, Bcr4Δ58-109-Strep or Bcr4Δ110-17-Strep) was loaded on Strep-Tactin beads, and then the beads were mixed with the lysate prepared from *E. coli* BL21, producing BscI-V5, respectively. After 3 h incubation at 4°C, the supernatant fraction (Sup) and pellet fraction (Pellet) samples were prepared. The Sup and Pellet samples were separated by SDS-PAGE and analyzed by Western blotting (WB) with anti-V5 antibody (top), and stained with Coomassie Brilliant Blue (CBB, bottom). Experiments were performed at least three times, and representative data are shown.

Fig. 2

bioRxiv preprint doi: https://doi.org/10.1101/2021.09.28.462275; this version posted August 9, 2022. The copyright holder for this preprint (which was not certified by peer review) is the author/funder, who has granted bioRxiv a license to display the preprint in perpetuity. It is made available under aCC-BY 4.0 International license.

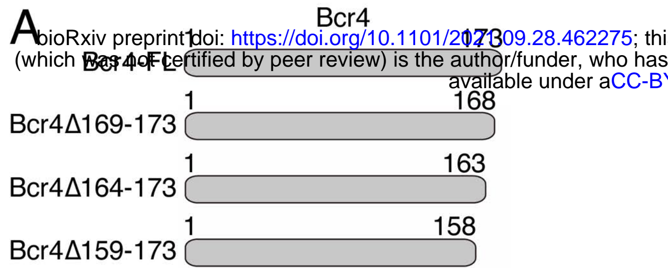

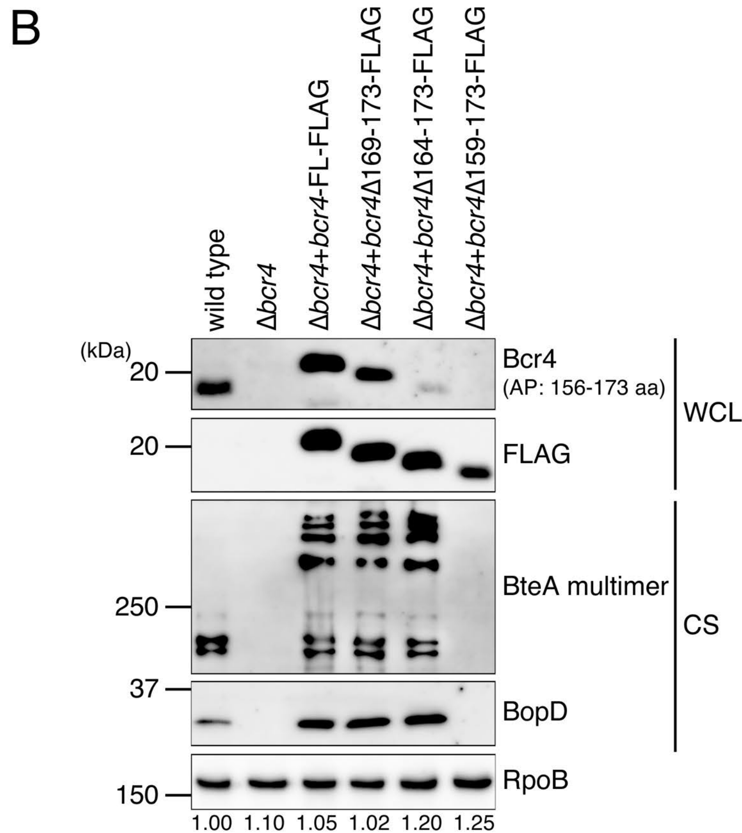

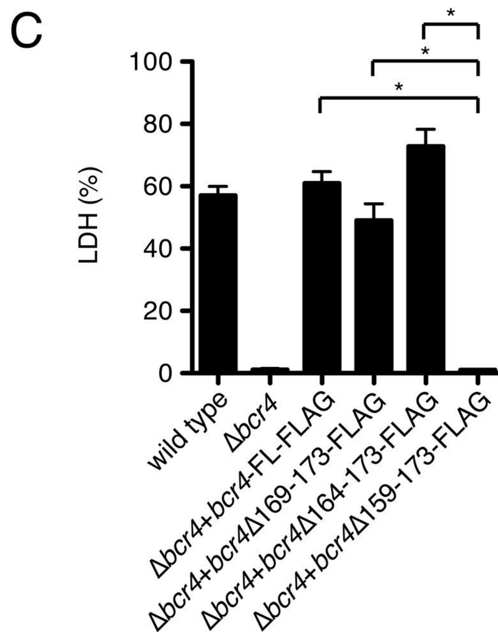

Fig. 3. The Bcr4 domain required for T3SS activity (A) Bcr4 derivatives used for the analysis of T3SS activity are depicted. (B) The *B. bronchiseptica* wild-type strain, Bcr4-deficient strain (Δ*bcr4*), and Δ*bcr4* producing Bcr4-FL-FLAG (Δ*bcr4*+*bcr4*-FL-FLAG), Bcr4Δ169-173-FLAG (Δ*bcr4*+*bcr4*Δ169-173-FLAG), Bcr4Δ164-173-FLAG (Δ*bcr4*+*bcr4* Δ164-173-FLAG), and Bcr4Δ159-173-FLAG (Δ*bcr4*+*bcr4*Δ159-173-FLAG) were cultured in SS medium. Whole cell lysates (WCL) and culture supernatant fraction (CS) samples were separated by SDS-PAGE and analyzed by Western blotting using antibodies against Bcr4, FLAG, BteA, BopD or RpoB. RpoB was used as an internal loading control. AP indicates the amino acids region of the antigen peptide used for anti-Bcr4 antibody generation. WCL and CS samples were prepared from equal volumes of bacterial culture. When we performed Western blotting using anti-BteA or BopD antibodies, we loaded a 100- or 50-fold smaller amount of Δ*bcr4*+*bcr4*-FL-FLAG, Δ*bcr4*+*bcr4*Δ169-173-FLAG and Δ*bcr4*+*bcr4*Δ164-173-FLAG CS samples on the SDS-PAGE gel than on the wild-type, Δ*bcr4* and Δ*bcr4*+*bcr4*Δ159-173-FLAG CS samples to avoid obtaining excess signal intensities. The numbers at the bottom of the lower panel indicate the relative signal intensity of RpoB measured using ImageJ software. (C) L2 cells were infected with each strain at an moi of 50 for 1 h. The amounts of LDH released into the extracellular medium from infected cells are shown, and the relative cytotoxicity (percent) was determined as described in the Materials and Methods. Error bars indicate the SEMs from triplicate experiments. *$P<0.05$. Experiments were performed at least three times, and representative data are shown.

Fig. 3

bioRxiv preprint doi: https://doi.org/10.1101/2021.09.28.462275; this version posted August 9, 2022. The copyright holder for this preprint (which was not certified by peer review) is the author/funder, who has granted bioRxiv a license to display the preprint in perpetuity. It is made available under aCC-BY 4.0 International license.

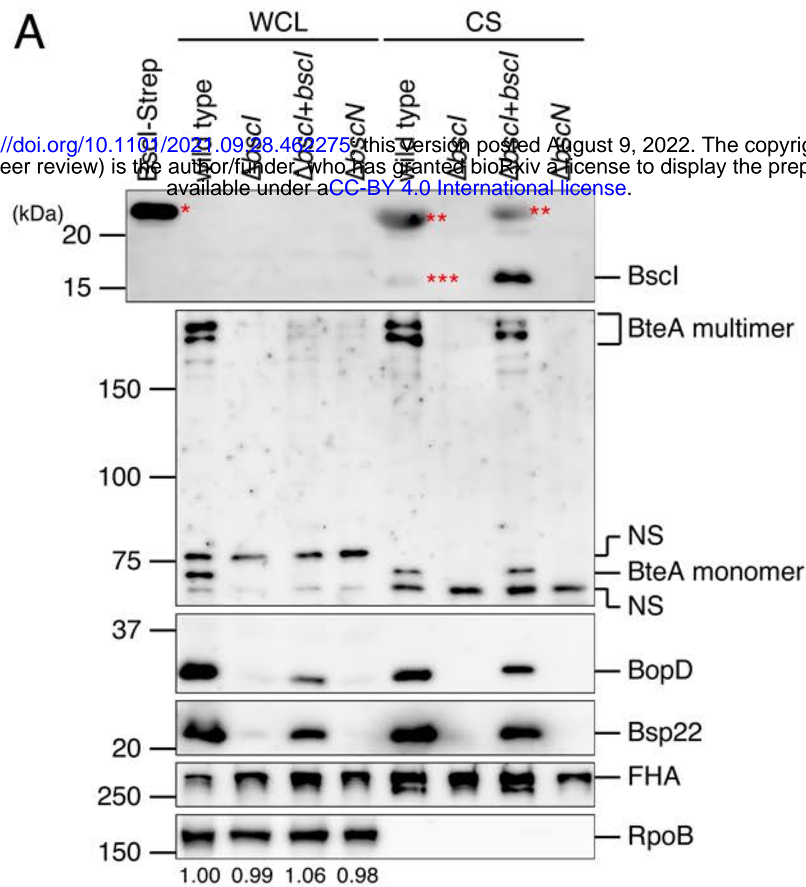

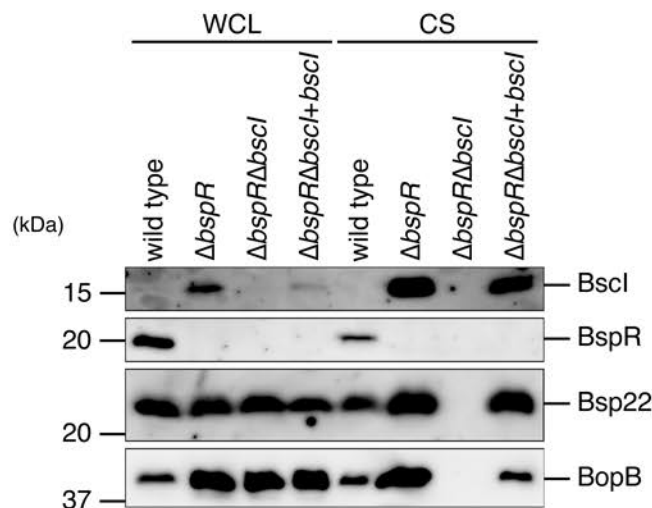

Fig. 4. The effect of BscI deletion on T3SS activity in *B. bronchiseptica*. (A) Whole cell lysates (WCL) and culture supernatant fraction (CS) samples were prepared from the wild-type strain, Δ*bscI* (BscI-deficient strain), Δ*bscI*+*bscI* (BscI-complemented strain) and Δ*bscN* (T3SS-inactive strain) cultured in SS medium. WCL and CS samples were separated by SDS-PAGE and analyzed by Western blotting using antibodies against BscI, BteA, BopD, Bsp22, FHA or RpoB. BscI tagged with Strep (BscI-Strep) was loaded as a control. *BscI-Strep signal; **NS (nonspecific signals); ***A faint signal of BscI. The numbers at the bottom of the lower panel indicate the relative signal intensity of RpoB measured using ImageJ software. (B) WCL and CS were prepared from the wild-type, Δ*bspR* (BspR-deficient strain), Δ*bspR*Δ*bscI* (BspR- and BscI-deficient strain) and Δ*bspR*Δ*bscI*+*bscI* (BscI-complemented BspR- and Bcr4-deficient strain) cultured in SS medium. WCL and CS were separated by SDS-PAGE and analyzed by Western blotting using antibodies against BscI, BspR, Bsp22 or BopB antibodies. Loaded WCL and CS samples were prepared from equal volumes of bacterial culture. When we performed Western blotting using antibodies against Bsp22 or BopB, we loaded a 25- or 5-fold smaller amount of Δ*bspR*, Δ*bspR*Δ*bscI* and Δ*bspR*Δ*bscI*+*bscI* WCL samples, and 5- or 10-fold smaller amount of Δ*bspR* and Δ*bspR*Δ*bscI*+*bscI* CS samples on the SDS-PAGE gel than the wild-type to avoid obtaining excess signal intensities. Experiments were performed at least three times, and representative data are shown.

Fig. 4

bioRxiv preprint doi: https://doi.org/10.1101/2021.09.28.462275; this version posted August 9, 2022. The copyright holder for this preprint (which was not certified by peer review) is the author/funder, who has granted bioRxiv a license to display the preprint in perpetuity. It is made available under aCC-BY 4.0 International license.

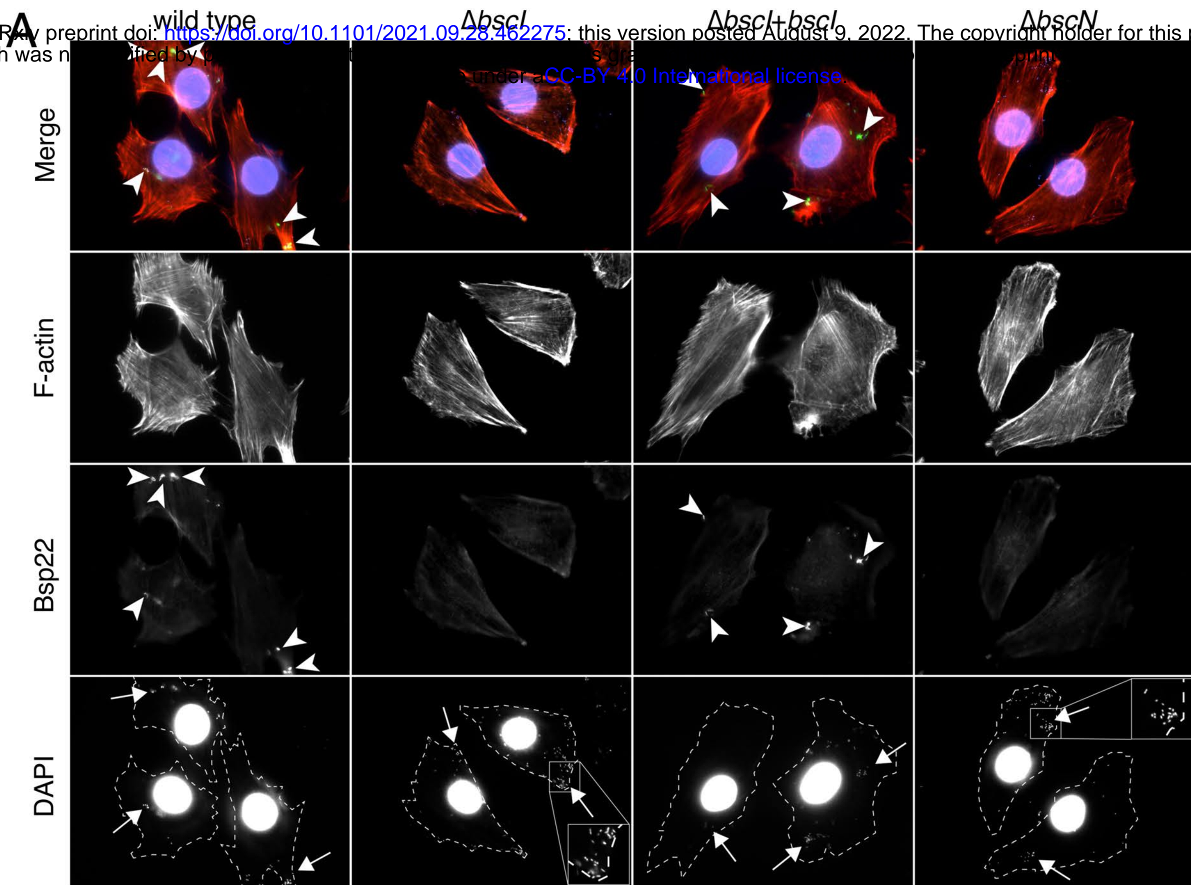

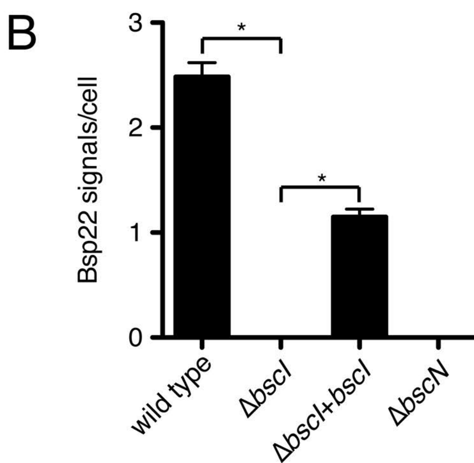

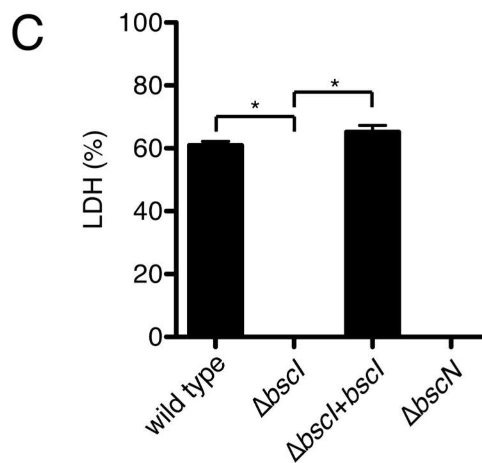

Fig. 5. Immunofluorescent staining of Bsp22 on L2 cells infected with *B. bronchiseptica* and the results of the LDH assay. (A) L2 cells were infected with the wild-type strain, Δ*bscI* (BscI-deficient strain), Δ*bscI*+*bscI* (BscI-complemented strain) or Δ*bscN* (T3SS-inactive strain) as described in the Materials and Methods. After fixation, cells were stained with anti-Bsp22 antibody (green), rhodamine phalloidin (red) and DAPI (blue). The inset shows higher magnification of the boxed area in the image. Arrowheads and arrows indicate the signals of Bsp22 (green) and bacteria, respectively. (B) Bsp22 signals per one cell were counted under a fluorescent microscope. At least 120 cells were randomly chosen. (C) The results of LDH assay at an MOI of 200 are shown as a histogram. Error bars indicate the SEMs from triplicate experiments. *P<0.05. Experiments were performed at least three times, and representative data are shown.

Fig. 5

bioRxiv preprint doi: https://doi.org/10.1101/2021.09.28.462275; this version posted August 9, 2022. The copyright holder for this preprint (which was not certified by peer review) is the author/funder, who has granted bioRxiv a license to display the preprint in perpetuity. It is made available under aCC-BY 4.0 International license.

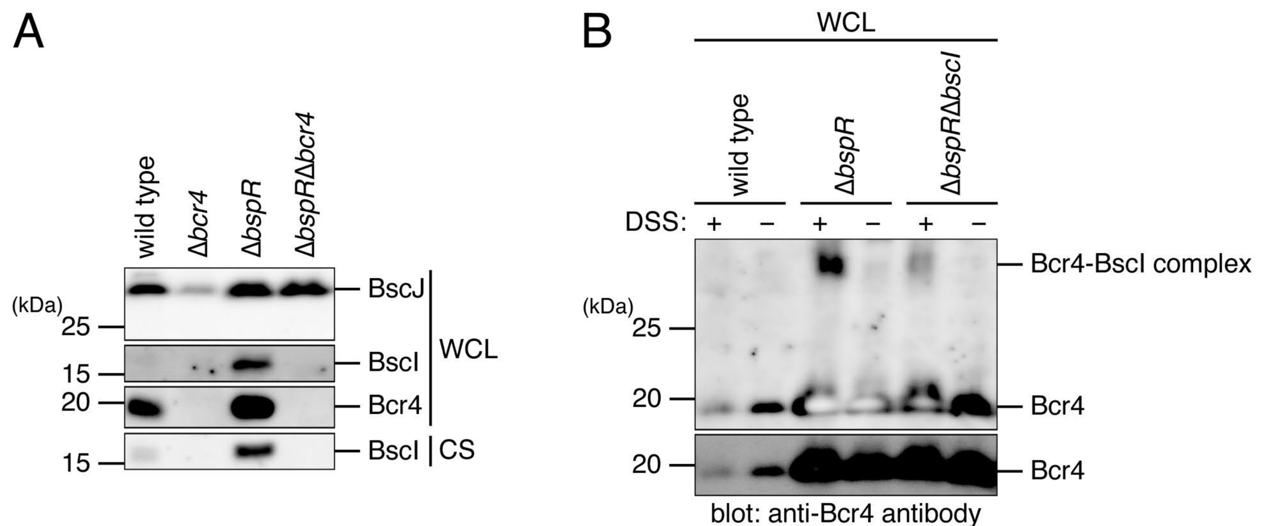

Fig. 6. The effect of Bcr4 on BscI stability and the suggestive interaction of Bcr4 with BscI in *B. bronchiseptica*. (A) The whole cell lysates (WCL) and culture supernatant fraction (CS) were prepared from the wild-type strain, Δ*bcr4* (Bcr4-deficient strain), Δ*bspR* (BspR-deficient strain) or Δ*bspR*Δ*bcr4* (BspR- and Bcr4-deficient strain) cultured in SS medium. WCL and CS were separated by SDS-PAGE and analyzed by Western blotting with antibodies against BscI (inner-rod protein), BscJ (inner-ring protein) and Bcr4. The samples were prepared from equal volumes of bacterial culture. When we carried out Western blotting using anti-BscJ or Bcr4 antibodies, we loaded a 10-fold-smaller amount of Δ*bspR* or Δ*bspR*Δ*bcr4* WCL samples on the SDS-PAGE than WT or Δ*bcr4* WCL samples to avoid obtaining excess signal intensities. (B) WCL were prepared from the wild-type, Δ*bspR* or Δ*bspR*Δ*bcr4* treated with (+) or without (–) cross linker disuccinimidyl suberate (DSS). WCL were separated by SDS-PAGE and analyzed by Western blotting with anti-Bcr4 antibody. The lower panel is a short exposure of the upper panel. Experiments were performed at least three times, and representative data are shown.

Fig. 6

bioRxiv preprint doi: https://doi.org/10.1101/2021.09.28.462275; this version posted August 9, 2022. The copyright holder for this preprint (which was not certified by peer review) is the author/funder, who has granted bioRxiv a license to display the preprint in perpetuity. It is made available under aCC-BY 4.0 International license.

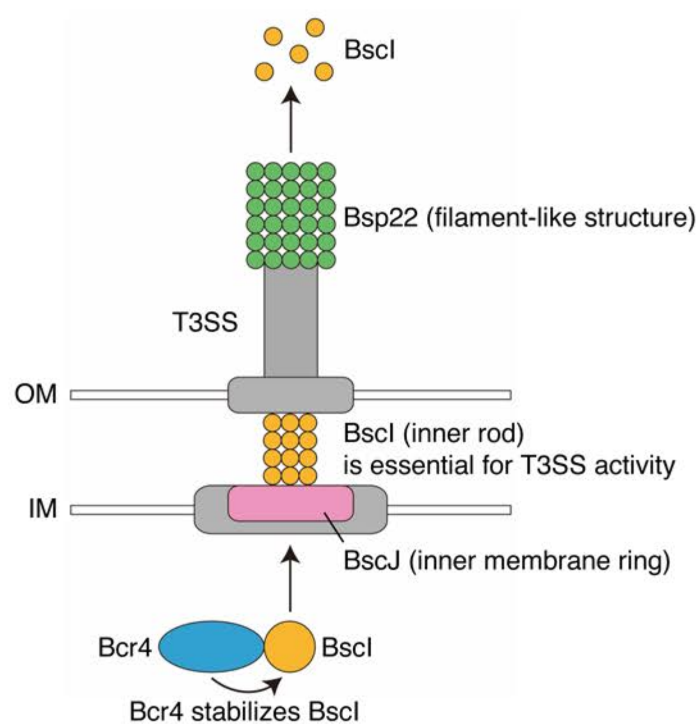

Fig. 7. Schematic depiction of the Bcr4 and BscI functions. In the *B. bronchiseptica* bacterial cytosol, Bcr4 (blue) stabilizes BscI (orange). Then, BscI is presumed to be localized to the T3SS machinery (gray) and form the inner rod. BscI is essential for T3SS activity and secreted from the bacterial cell. BscJ (pink) is predicted to function as an inner membrane ring. Bsp22 (green) forms a filament-like structure. OM and IM indicate the outer membrane (white) and inner membrane (white), respectively.

Fig. 7

bioRxiv preprint doi: https://doi.org/10.1101/2021.09.28.462275; this version posted August 9, 2022. The copyright holder for this preprint (which was not certified by peer review) is the author/funder, who has granted bioRxiv a license to display the preprint in perpetuity. It is made available under aCC-BY 4.0 International license.

Supplemental material

Text S. Supplementary Information

Fig. S1. Construction of the T3SS machinery in strains lacking Bcr4 and/or BspR. In the *B. bronchiseptica* wild-type (upper left), the BspR negative regulation level for the *bsc* locus transcription is moderate, and the T3SS machinery is established. In the Bcr4-deficient strain (upper right), BspR strongly represses the *bsc* locus transcription, and construction of the T3SS machinery is incomplete. In the BspR-deficient strain (lower left), the negative regulatory effect of BspR is cancelled, and the construction of the T3SS machinery is promoted. In the BspR/Bcr4 double-deficient strain (lower right), while the *bsc* locus transcription is promoted because of BspR deficiency, T3SS is not functional.

Fig. S2. Alignment of Bcr4 amino acid sequences in representative *Bordetella* species. Bcr4 amino acid sequences of *B. bronchiseptica* S798 (Bb), *B. pertussis* Tohama I (Bp) and *B. parapertussis* 12822 (Bp) were compared using ClustalW. The grey highlighted letters represent amino acid residues that were different from those in Bb. Bcr4 of Bp and Bpp have 98.3% and 97.1% identities with those of Bp, respectively.

Fig. S3. The nonspecific reaction of anti-BscI antibody to Bsp22. The culture supernatants (CS) were prepared from the wild-type strain, Δ*bsp22* (Bsp22-deficient strain),

bioRxiv preprint doi: https://doi.org/10.1101/2021.09.28.462275; this version posted August 9, 2022. The copyright holder for this preprint (which was not certified by peer review) is the author/funder, who has granted bioRxiv a license to display the preprint in perpetuity. It is made available under aCC-BY 4.0 International license.

21 Δ*bspR* (BspR-deficient strain) or Δ*bscI*+*bscI* (BscI-complemented strain) cultured in SS

22 medium. The CS samples were separated by SDS-PAGE and stained with Coomassie

23 Brilliant Blue (CBB, left panel) or analyzed by Western blotting (WB) with anti-BscI antibody

24 (right panel). NS indicates nonspecific signals. Experiments were performed at least three

25 times, and representative data are shown.

26

27 **Fig. S4. The results of the RT-PCR analysis for the mRNA level of *bscI* in *B.***

28 ***bronchiseptica* strains.** Total RNA was prepared from the wild-type strain, Δ*bspR* (BspR-

29 deficient strain) or Δ*bspR*Δ*bcr4* (BspR- and Bcr4-deficient strain) cultured in SS medium and

30 subjected to a quantitative RT-PCR analysis. The histogram shows the relative amount of

31 *bscI* mRNA normalized by the housekeeping gene, *recA* mRNA. Experiments were

32 performed at least three times, and representative data are shown.

33

34 **Fig. S5. The results of the RT-PCR analysis for mRNA levels of *bopD* and *bscI* in the**

35 **wild-type *B. bronchiseptica*.** Total RNA was prepared from the wild-type strain cultured in

36 SS medium and subjected to a quantitative RT-PCR analysis. The histogram shows the

37 relative amount of *bopD* and *bscI* mRNA in the wild-type. The relative ratio of *bscI* mRNA is

38 shown when the *bopD* mRNA amount is set as 1. Experiments were performed at least three

39 times, and representative data are shown.

40

bioRxiv preprint doi: https://doi.org/10.1101/2021.09.28.462275; this version posted August 9, 2022. The copyright holder for this preprint (which was not certified by peer review) is the author/funder, who has granted bioRxiv a license to display the preprint in perpetuity. It is made available under aCC-BY 4.0 International license.

41

42 **Fig. S6. The time course of BscI production in *B. bronchiseptica*.** The whole cell lysates
43 (WCL) were prepared from the wild-type strain, Δ*bcr4* (Bcr4-deficient strain), Δ*bspR* (BspR-
44 deficient strain) or Δ*bspR*Δ*bcr4* (BspR- and Bcr4-deficient strain) cultured in SS medium for
45 0, 2, 5, 8 or 18 hr. The WCL were separated by SDS-PAGE and analyzed by Western blotting
46 with antibodies against BscI, BopB and RpoB. Experiments were performed at least three
47 times, and representative data are shown.

48

49 **Fig. S7. The predicted structural model of *B. bronchiseptica* Bcr4**
50 (A) The AlphaFold2 (AF2)-predicted structural model of *B. bronchiseptica* Bcr4 and
51 structural comparison with *Aeromonas hydrophila* AcrH (PDB: 3WXX) and *Pseudomonas*
52 *aeruginosa* PscG (PDB: 2UWJ). Z-score, root mean square deviation (RMSD), and amino
53 acid identity (AA %ID) of AcrH and PscG compared with Bcr4 are shown, respectively. (B)
54 The pairwise sequence alignment of Bcr4, AcrH, and PscG. The most frequent amino acid
55 type is colored. The secondary structure assignments (H/h: helix, E/e: strand, L/l: coil) are
56 also shown.

57

58

59

60

bioRxiv preprint doi: https://doi.org/10.1101/2021.09.28.462275; this version posted August 9, 2022. The copyright holder for this preprint (which was not certified by peer review) is the author/funder, who has granted bioRxiv a license to display the preprint in perpetuity. It is made available under aCC-BY 4.0 International license.

61 **Table S1. Nomenclature of the *Bordetella* T3SS component**

62

63 **Table S2. Plasmids used in the study**

64

65 **Table S3. Primers used in the study**

66

67

68

69

70

71

72

73

74

75

76

77

78

79

80

bioRxiv preprint doi: https://doi.org/10.1101/2021.09.28.462275; this version posted August 9, 2022. The copyright holder for this preprint (which was not certified by peer review) is the author/funder, who has granted bioRxiv a license to display the preprint in perpetuity. It is made available under aCC-BY 4.0 International license.

81 **Supplementary Information**

82 SI Materials and Methods

83 Pull-down assay.

84 The plasmids and primers used in this study are listed in Table S1 and S2, respectively.
85 In order to express *bscI*, *bscK*, *bscJ* or *bcr4* tagged with a V5 sequence at the respective C-
86 terminus (*bscI*-V5, *bscK*-V5, *bscJ*-V5 or *bcr4*-V5), we amplified DNA fragments encoding
87 the *bscI*, *bscK*, *bscJ* or *bcr4* genes with the primer sets of B1-bscI-V5 and B2-bscI-V5, B1-
88 bscK-V5 and B2-bscK-V5, B1-bscJ-V5 and B2-bscJ-V5 or B1-bcr4-comp and B2-bcr4-V5,
89 respectively, using *B. bronchiseptica* S798 genomic DNA as the template. Each resulting
90 PCR product was cloned into pDONR201 to obtain pMGKU404, pMGKU405, pMGKU406
91 or pMGKU407, respectively, by means of adapter PCR and site-specific recombination
92 techniques using the Gateway cloning system (Invitrogen). Each plasmid was mixed with an
93 expression vector such as p99*ccdB*-V5 (1) to obtain pMGKU408, pMGKU409, pMGKU410
94 or pMGKU411 using the Gateway cloning system.

95 BL21 cells carrying pMGKU408, pMGKU409 pMGKU410 or pMGKU411 were cultured
96 overnight at 37ºC with shaking, and then diluted 1:40 in LB liquid medium containing 50
97 *μ*L/mL ampicillin and incubated for 2 h at 37ºC with shaking. Each bacterial culture was
98 further incubated for 5 h at 30ºC in the presence of isopropyl-beta-thiogalactopyranoside
99 (IPTG) at the final concentration of 1 mM. Bacteria were collected by centrifugation at
100 2,600×*g* for 15 min, and suspended in cold TBS containing protease inhibitor cocktail,

bioRxiv preprint doi: https://doi.org/10.1101/2021.09.28.462275; this version posted August 9, 2022. The copyright holder for this preprint (which was not certified by peer review) is the author/funder, who has granted bioRxiv a license to display the preprint in perpetuity. It is made available under aCC-BY 4.0 International license.

101 cOmplete (Roche). Each bacterial suspension was sonicated, and each supernatant was
102 used for the pull-down assay.

103 Next, in order to purify Bcr4 or BscI tagged with six histidine residues (6×His) at the
104 respective N-terminus and Strep at the respective C-terminus, we amplified DNA fragments
105 encoding *bcr4* or *bscI* with the primer sets of 5-HindIII-bcr4 and 3-bcr4-Strep, or 5-HindIII-
106 bscI and 3-bscI-Strep using *B. bronchiseptica* S798 genomic DNA as the template. Each
107 amplified DNA fragment was used as a template for 2nd PCR with a primer set consisting
108 of the upper primer used in the 1st PCR and 3-Strep-HindIII to add a 24 bp sequence
109 encoding the Strep tag. Each resulting PCR product was cloned into the HindIII recognition
110 sites of pColdII to obtain pMGKU412 or pMGKU413 by the In-Fusion Cloning System
111 (Clontech), respectively. In order to purify Bcr4 lacking the amino acids region 58–109 or
112 110–173, we amplified the DNA fragment with the primer sets of 5-bcr4-58-109-Strep-IF and
113 3-IF-bcr4-58-109-Strep, or 5-bcr4-110-173-Strep-IF and 3-IF-bcr4-110-173-Strep using
114 pColdII-*bcr4*-Strep as the template. Each amplified fragment was self-ligated by the In-
115 Fusion Cloning System, respectively, and then designated pMGKU414 or pMGKU415.

116 BL21 cells carrying pMGKU412, pMGKU413, pColdII-*bteA*-N-Strep (2), pMGKU414 or
117 pMGKU415 were cultured overnight at 37ºC with shaking, and then diluted 1:100 in LB liquid
118 medium containing 50 μL/mL ampicillin and incubated for 2 h at 37ºC with shaking,
119 respectively. Each bacterial culture was further incubated overnight at 15ºC in the presence
120 of IPTG at the final concentration of 0.05 mM. Bacteria were collected by centrifugation at

bioRxiv preprint doi: https://doi.org/10.1101/2021.09.28.462275; this version posted August 9, 2022. The copyright holder for this preprint (which was not certified by peer review) is the author/funder, who has granted bioRxiv a license to display the preprint in perpetuity. It is made available under aCC-BY 4.0 International license.

121 2,600×*g* for 20 min, and suspended in cold TBS containing cOmplete. Each bacterial
122 suspension was sonicated and each supernatant except for that of pMGKU413 was
123 subjected to purification using Ni-NTA agarose (Qiagen) according to the manufacturer's
124 instructions. The purified proteins were dialyzed with TBS. As for pMGKU413, the bacterial
125 suspension was sonicated and the pellet was suspended in Inclusion Body Solubilization
126 Reagent (Thermo) according to the manufacturer's instructions. The BscI-Strep in
127 solubilized solution was refolded as described previously (3). Briefly, the solubilized solution
128 was diluted with 5-fold larger refolding buffer (20 mM Tris-HCl, pH-8, 150 mM NaCl, 10%
129 glycerol) overnight at 4°C on a rotator, and then centrifugated at 20,000×*g* for 15 min. The
130 supernatant was dialyzed with dialysis buffer (20 mM Tris-HCl, pH-8, 150 mM NaCl, 10%
131 glycerol), and then centrifugated at 20,000×*g* for 15 min. The supernatant was used as
132 purified protein for the pull-down assay.

133 We mixed the dual-tagged protein (6×His and Strep) and 30 μl Strep-Tactin resin (IBA) in
134 an Eppendorf tube and rotated the tube at 4°C for 1 h. Then, we washed the beads with
135 TBS three times. Next, the V5-tagged protein-containing *E. coli* lysate was added to the tube
136 and rotated at 4°C for 3 h. We transferred 30 μL supernatant to new Eppendorf tube and
137 added 30 μL 2×SDS-PAGE sample buffer to prepare the Sup. Then we washed the beads
138 with TBS (Fig. 1B and 1C) or TBS containing 0.1% Triton X-100 (Fig. 1C) three times and
139 added 30 μL 2×SDS-PAGE sample buffer to prepare the Pellet samples.

140

bioRxiv preprint doi: https://doi.org/10.1101/2021.09.28.462275; this version posted August 9, 2022. The copyright holder for this preprint (which was not certified by peer review) is the author/funder, who has granted bioRxiv a license to display the preprint in perpetuity. It is made available under aCC-BY 4.0 International license.

141 **Construction of a *bscI* gene-disrupted or *bspR*/*bscI* double strains.**

142 To construct the *bscI* or *bspR*/*bscI* double mutants, a 2.4 kb DNA fragment encoding *bscI*
143 and its flanking regions was amplified by PCR with primers B1-bscI and B2-bscI using *B.*
144 *bronchiceptica* S798 genomic DNA as the template. The resulting PCR product was cloned
145 into pDONR201 to obtain pMGKU416 using the Gateway cloning system. An inverse PCR
146 was carried out with the primers R1-bscI and R2-bscI using circular pMGKU416 as the
147 template. The resulting PCR product was self-ligated using the In-Fusion Cloning System to
148 obtain pMGKU417. This plasmid contained a 369-bp in-frame deletion from 30 bp
149 downstream of the 5' end of the *bscI* gene to 30 bp upstream of the 3' end of the gene. This
150 plasmid, pMGKU417, was mixed with a positive suicide vector such as pABB-CRS2 (4) to
151 obtain pMGKU418 using the Gateway cloning system. The pMGKU418 or pABB-CRS2-
152 *bspR* (5) plasmids in turn were introduced into *E. coli* Sm10λ*pir*, and transconjugated into
153 the S798 wild-type or Δ*bscI* as described previously (6). The resulting mutant strains were
154 designated Δ*bscI* or Δ*bspR*Δ*bscI*, respectively.

155

156 **Construction of plasmids used for producing Bcr4 derivatives and BscI**
157 **complementation**

158 In order to produce full-length Bcr4 tagged with a FLAG sequence at the C-terminus, we
159 performed an inverse PCR with primers of 5-bcr4-FLAG-IF and 3-IF-bcr4-FLAG using
160 pDONR-*bcr4* (7) as the template. The resulting PCR product was self-ligated to obtain

bioRxiv preprint doi: https://doi.org/10.1101/2021.09.28.462275; this version posted August 9, 2022. The copyright holder for this preprint (which was not certified by peer review) is the author/funder, who has granted bioRxiv a license to display the preprint in perpetuity. It is made available under aCC-BY 4.0 International license.

161 pMGKU419 by the In-Fusion Cloning System. To produce Bcr4 lacking the amino acid
162 regions 159–173, 164–173 or 169–173, inverse PCR was carried out with the primer sets of
163 5-*bcr4*-FLAG-IF and 3-IF-bcr4Δ169-173-FLAG, 5-*bcr4*-FLAG-IF and 3-IF-*bcr4*Δ164-173-
164 FLAG, or 5-*bcr4*-FLAG-IF and 3-IF-*bcr4*Δ159-173-FLAG using pMGKU419 as the template.
165 Each amplified fragment was self-ligated by the In-Fusion Cloning System to obtain
166 pMGKU420, pMGKU421 or pMGKU422, respectively. For BscI complementation, a PCR
167 was carried out with the primers of B1-bscI-V5 and 3-B2-bscI-comp using *B. bronchiceptica*
168 S798 genomic DNA as the template. The resulting PCR product was cloned into pDONR201
169 to obtain pMGKU423 using the Gateway cloning system. These plasmids were mixed with
170 pRK-R4-R3-F, pDONR-*fha*P and pDONR-*rrnB* (8) to obtain pMGKU424*,* pMGKU425,
171 pMGKU426*,* pMGKU427 and pMGKU428 using the Gateway cloning system.

172

173 **Quantitative reverse transcription-PCR**

174 Total RNA was prepared from the *B. bronchiseptica* culture using a Trizol Max Bacterial RNA
175 isolation Kit (Invitrogen), RNeasy Mini Kit (Qiagen), and RNase-free DNase Kit (Qiagen).
176 The reverse transcription reaction was carried out using Transcriptor Universal cDNA Master
177 (Roche) and T100 Thermal Cycler (Bio-Rad). The quantitative RT-PCR reaction was carried
178 out using FastStart Essential DNA Probes Master (Roche) and Light Cycler 96 (Roche). To
179 amplify the *bscI*, *bopD*, and *recA* genes, the primer sets 5-bscI and 3-bscI, 5-bopD and 3-
180 bopD, 5-recA and 3-recA were used, respectively. For the experiment to determine the

bioRxiv preprint doi: https://doi.org/10.1101/2021.09.28.462275; this version posted August 9, 2022. The copyright holder for this preprint (which was not certified by peer review) is the author/funder, who has granted bioRxiv a license to display the preprint in perpetuity. It is made available under aCC-BY 4.0 International license.

181 presence of *bscI* mRNA in the Bcr4 mutant (Fig. S4); *recA* was used as an internal control.
182 The values obtained from each strain were standardized with *recA*, and the relative amounts
183 to the wild-type strain were determined. For the experiment to compare the amounts of *bscI*
184 and *bopD* mRNA in the wild-type (Fig. S5), we followed the protocol provided by Roche. The
185 genome of *B. bronchiseptica* was used as a template for quantitative RT-PCR to generate a
186 calibration curve. The relative amount of *bopD* mRNA to *bscI* mRNA was then determined
187 using the calibration curve.
188

189 **Protein structure prediction**

190 Protein structure prediction using amino acid sequences by AlphaFold2 with MMseqs2
191 (ColabFold) was performed on the Google Colab server with default parameters (9). A
192 structure-based protein homology search using AlphaFold2-predicted structural models was
193 performed on the Dali server (10). In addition, primary, secondary, and tertiary structures of
194 query proteins were visualized and compared with those of neighbors on the Dali server.
195
196
197
198
199
200

bioRxiv preprint doi: https://doi.org/10.1101/2021.09.28.462275; this version posted August 9, 2022. The copyright holder for this preprint (which was not certified by peer review) is the author/funder, who has granted bioRxiv a license to display the preprint in perpetuity. It is made available under aCC-BY 4.0 International license.

201 **References**

202 1. Ogino T, Ohno R, Sekiya K, Kuwae A, Matsuzawa T, Nonaka T, Fukuda H, Imajoh-
203 Ohmi S, Abe A. 2006. Assembly of the type III secretion apparatus of
204 enteropathogenic *Escherichia coli*. J Bacteriol 188:2801-11.
205 2. Kuwae A, Momose F, Nagamatsu K, Suyama Y, Abe A. 2016. BteA Secreted from the
206 *Bordetella bronchiseptica* Type III Secetion System Induces Necrosis through an
207 Actin Cytoskeleton Signaling Pathway and Inhibits Phagocytosis by Macrophages.
208 PLoS One 11:e0148387.
209 3. Halder PK, Roy C, Datta S. 2019. Structural and functional characterization of type
210 three secretion system ATPase PscN and its regulator PscL from *Pseudomonas*
211 *aeruginosa*. Proteins 87:276-288.
212 4. Sekiya K, Ohishi M, Ogino T, Tamano K, Sasakawa C, Abe A. 2001. Supermolecular
213 structure of the enteropathogenic *Escherichia coli* type III secretion system and its
214 direct interaction with the EspA-sheath-like structure. Proc Natl Acad Sci U S A
215 98:11638-43.
216 5. Kurushima J, Kuwae A, Abe A. 2012. The type III secreted protein BspR regulates
217 the virulence genes in *Bordetella bronchiseptica*. PLoS One 7:e38925.
218 6. Donnenberg MS, Kaper JB. 1991. Construction of an eae deletion mutant of
219 enteropathogenic *Escherichia coli* by using a positive-selection suicide vector. Infect
220 Immun 59:4310-7.

bioRxiv preprint doi: https://doi.org/10.1101/2021.09.28.462275; this version posted August 9, 2022. The copyright holder for this preprint (which was not certified by peer review) is the author/funder, who has granted bioRxiv a license to display the preprint in perpetuity. It is made available under aCC-BY 4.0 International license.

221 7. Nishimura R, Abe A, Sakuma Y, Kuwae A. 2018. *Bordetella bronchiseptica* Bcr4
222 antagonizes the negative regulatory function of BspR via its role in type III secretion.
223 Microbiol Immunol 62:743-754.
224 8. Kuwae A, Matsuzawa T, Ishikawa N, Abe H, Nonaka T, Fukuda H, Imajoh-Ohmi S,
225 Abe A. 2006. BopC is a novel type III effector secreted by *Bordetella bronchiseptica*
226 and has a critical role in type III-dependent necrotic cell death. J Biol Chem 281:6589-
227 600.
228 9. Mirdita M, Schutze K, Moriwaki Y, Heo L, Ovchinnikov S, Steinegger M. 2022.
229 ColabFold: making protein folding accessible to all. Nat Methods 19:679-682.
230 10. Holm L. 2020. Using Dali for Protein Structure Comparison. Methods Mol Biol
231 2112:29-42.
232

bioRxiv preprint doi: https://doi.org/10.1101/2021.09.28.462275; this version posted August 9, 2022. The copyright holder for this preprint (which was not certified by peer review) is the author/funder, who has granted bioRxiv a license to display the preprint in perpetuity. It is made available under aCC-BY 4.0 International license.

Table S1. Nomencalture of the *Bordetella* T3SS

Unified name	*Bordetella*	*Yersinia*	*Pseudomonas*	Predicted function
SctF	BscF	YscF	PscF	Needle
SctI	BscI	YscI	PscI	Inner rod
SctE	BopB	YopB	PopB	Translocation pore
SctB	BopD	YopD	PopD	Translocation pore
SctA	Bsp22	LcrV	PcrV	Needle tip or Filament
SctJ	BscJ	YscJ	PscJ	Inner membrane ring
SctK	BscK	YscK	PscK	ATPase cofactor
SctN	BscN	YscN	PscN	ATPase

bioRxiv preprint doi: https://doi.org/10.1101/2021.09.28.462275; this version posted August 9, 2022. The copyright holder for this preprint (which was not certified by peer review) is the author/funder, who has granted bioRxiv a license to display the preprint in perpetuity. It is made available under aCC-BY 4.0 International license.

Table S2. Plasmids used in the study

Name	Description	Reference or source
pDONR201	DNA cloning vector, Km^r	Invitrogen
pMGKU404	pDONR201, *bscI* gene tagged with V5 sequence at the C terminus	This study
pMGKU405	pDONR201, *bscK* gene tagged with V5 sequence at the C terminus	This study
pMGKU406	pDONR201, *bscJ* gene tagged with V5 sequence at the C terminus	This study
pMGKU407	pDONR201, *bcr4* gene tagged with V5 sequence at the C terminus	This study
p99*ccdB*-V5	Expression vector for V5 tagged gene, Amp^r	1
pMGKU408	p99-*ccdB*-V5, *bscI* gene tagged with V5 sequence at the C terminus	This study
pMGKU409	p99-*ccdB*-V5, *bscK* gene tagged with V5 sequence at the C terminus	This study
pMGKU410	p99-*ccdB*-V5, *bscJ* gene tagged with V5 sequence at the C terminus	This study
pMGKU411	p99-*ccdB*-V5, *bsc4* gene tagged with V5 sequence at the C terminus	This study
pColdII	Expression vector for His tagged gene, Amp^r	TAKARA
pMGKU412	pColdII, *bcr4* gene tagged with Strep sequence at the C terminus	This study
pMGKU413	pColdII, *bscI* gene tagged with Strep sequence at the C terminus	This study
pMGKU414	pColdII, *bcr4* gene lacking amino acids region 58-109 tagged with Strep sequence at the C terminus	This study
pMGKU415	pColdII, *bcr4* gene lacking amino acids region 110-173 tagged with Strep sequence at the C terminus	This study
pColdII-*bteA*-N-Strep	pColdII, *bteA* gene coding amino acids region 1-312 tagged with Strep sequence at the C terminus	2
pMGKU416	pDONR201, *bscI* gene	This study
pMGKU417	pDONR201, *bscI* gene containing internal sequence-deletion and its flanking region	This study
pABB-CRS2	Suicide vector for conjugation, Amp^r	4
pMGKU418	pABB-CRS2, *bscI* gene containing internal sequence-deletion and its flanking region	This study
pABB-CRS2-*bspR*	pABB-CRS2, *bspR* gene containing internal sequence-deletion and its flanking region	5
pDONR-*bcr4*	pDONR201, *bcr4* gene for complementation	7
pMGKU419	pDONR201, *bcr4* gene tagged with FLAG sequence at the C terminus for complementation	This study
pMGKU420	pDONR201, *bcr4* gene lacking amino acids region 169-173 tagged with FLAG sequence at the C terminus	This study
pMGKU421	pDONR201, *bcr4* gene lacking amino acids region 164-173 tagged with FLAG sequence at the C terminus	This study
pMGKU422	pDONR201, *bcr4* gene lacking amino acids region 159-173 tagged with FLAG sequence at the C terminus	This study
pMGKU423	pDONR201, *bscI* gene for complementation	This study
pRK415-R4-R3-F	pRK415, recombination sites for MultiSite Gateway, Tet^r	8
pDONR-*fhaP*	pDONR-P4-P1R, *fha* promoter	8
pDONR-*rrnB*	pDONR-P2R-P3, *rrnB* terminator	8
pMGKU424	pRK415-R4-R3-F, *bcr4* gene tagged with FLAG sequence at the C terminus for complementation	This study
pMGKU425	pRK415-R4-R3-F, *bcr4* gene lacking amino acids region 169-173 tagged with FLAG sequence at the C terminus	This study
pMGKU426	pRK415-R4-R3-F, *bcr4* gene lacking amino acids region 164-173 tagged with FLAG sequence at the C terminus	This study
pMGKU427	pRK415-R4-R3-F, *bcr4* gene lacking amino acids region 159-173 tagged with FLAG sequence at the C terminus	This study
pMGKU428	pRK415-R4-R3-F, *bscI* gene	This study

bioRxiv preprint doi: https://doi.org/10.1101/2021.09.28.462275; this version posted August 9, 2022. The copyright holder for this preprint (which was not certified by peer review) is the author/funder, who has granted bioRxiv a license to display the preprint in perpetuity. It is made available under aCC-BY 4.0 International license.

Table S3. Primers used in the study

Name	Sequence (5'→3')
B1-bscI-V5	AAAAAGCAGGCTTGTTGGACAGCGGACCCGCC
B2-bscI-V5	AGAAAGCTGGGTTTGACATTCTCGCCAGCGTGTC
B1-bscK-V5	AAAAAGCAGGCTTGGCGCACGCGCTGGTCCCG
B2-bscK-V5	AGAAAGCTGGGTTGGCTTGGGCGGGGAACGAGG
B1-BscJ-V5	AAAAAGCAGGCTTGGAGTACGAGTTGGTGGGC
B2-BscJ-V5	AGAAAGCTGGGTTGTCATGCCCGGCTCCTTCCG
B1-bcr4-comp	AAAAAGCAGGCTGCCAGGTCCGGTCTCGCACCG
B2-bcr4-V5	AGAAAGCTGGGTTTCCAGGAGCTCCAGGTAATG
5-HindIII-bcr4	ATCCGAATTCAAGCTTCATTCAGACTCAGGTTCAGATTC
3-bcr4-Strep	CGGGTGGCTCCATCCAGGAGCTCCAGGTAATG
5-HindIII-bscI	ATCCGAATTCAAGCTTAATTTGGATCTGACGGCGATC
3-bscI-Strep	CGGGTGGCTCCATGACATTCTCGCCAGCGTGTC
3-Strep-HindIII	GCAGGTCGACAAGCTTTCATTTTTCGAACTGCGGGTGGCTCCA
5-bcr4-58-109-Strep-IF	GCCGTCAGCGATCTGTCGGACTGGACGCCTGGTG
3-IF-bcr4-58-109-Strep	CAGATCGCTGACGGCCGCCG
5-bcr4-110-173-Strep-IF	TGGAGCCACCCGCAGTTCGA
3-IF-bcr4-110-173-Strep	CTGCGGGTGGCTCCAGCGGTCCTCCGCCTGTGCCG
B1-bscI	AAAAAGCAGGCTTCATGACTGTTCACGACGAC
B2-bscI	AGAAAGCTGGGTGCACAAGATCCAGCGCGACC
R1-bscI	CGACGTTGGCGTTGATCGCCGTCAGATC
R2-bscI	TCAACGCCAACGTCGACACGCTGGCGAG
5-bcr4-FLAG-IF	CCACCCGCAGTTCGAAAAATGAATTTGGATCTACCCAGCTTTCTTG
3-IF-bcr4-FLAG	TCGAACTGCGGGTGGCTCCATCCAGGACCTCCAGGTAATGGCTCG
3-IF-bcr4Δ169-173-FLAG	GTCATCCTTGTAGTCTAATGGCTCGGACTGCAACG
3-IF-bcr4Δ164-173-FLAG	GTCATCCTTGTAGTCCAACGGCGCGGGCCGCATCATG
3-IF-bcr4Δ159-173-FLAG	GTCATCCTTGTAGTCCATCATGGCGGGTCCGCTGTC
3-B2-bscI-comp	AGAAAGCTGGGTTTGACATTCTCGCCAGCGTGTC
5-bscI	CGATCTGCAGGCCAGGTT
3-bscI	CTATTGCCTTGCCCACCAA
5-bopD	CGGCTCGGTGAAGACATC
3-bopD	CCTCCCGCATCTGTTGAC
5-recA	ATGAAGATCGGCGTGATGT
3-recA	TAGAACTTGAGCGCGTTGC

bioRxiv preprint doi: https://doi.org/10.1101/2021.09.28.462275; this version posted August 9, 2022. The copyright holder for this preprint (which was not certified by peer review) is the author/funder, who has granted bioRxiv a license to display the preprint in perpetuity. It is made available under aCC-BY 4.0 International license.

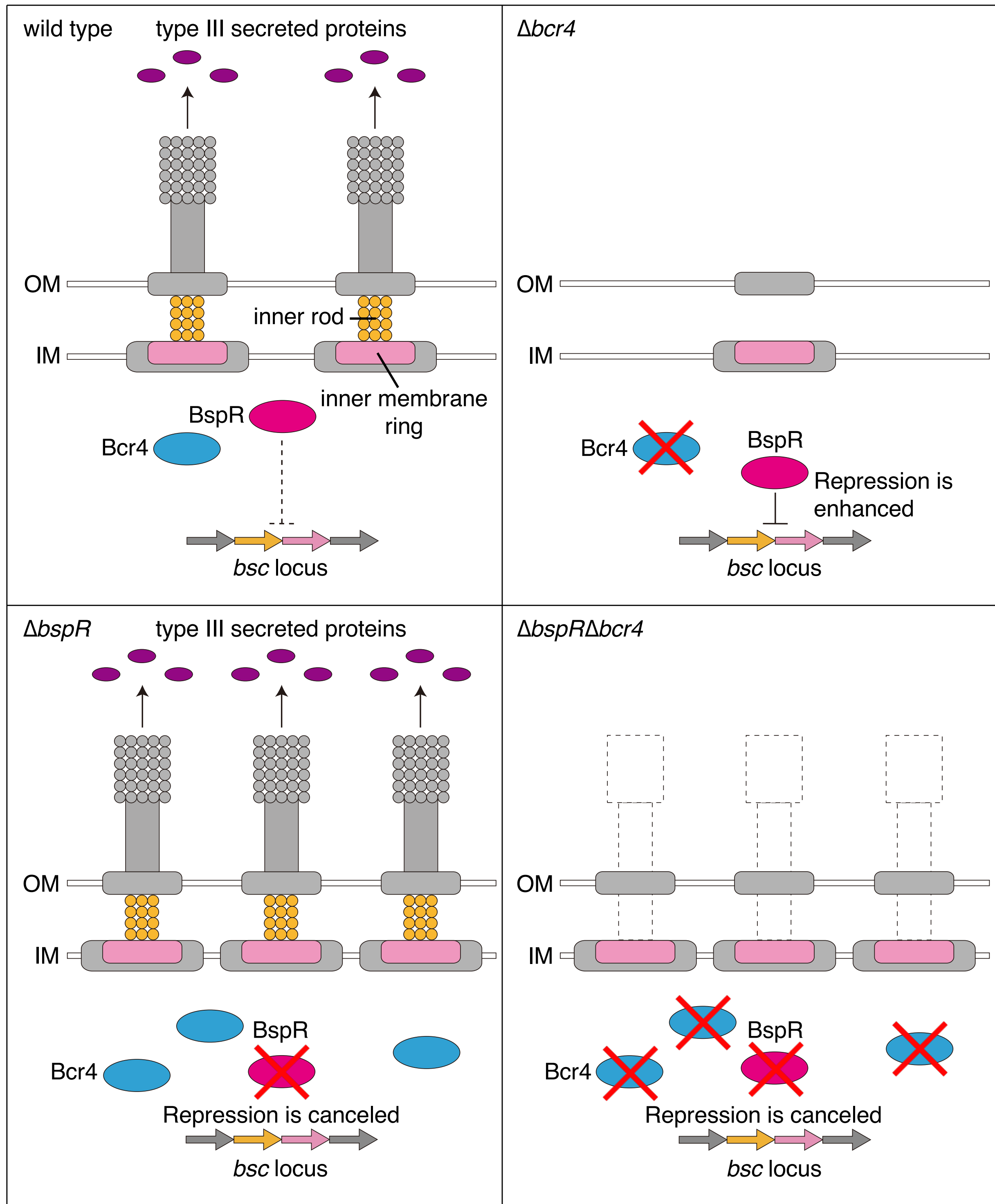

Fig. S1. Construction of the T3SS machinery in strains lacking Bcr4 and/or BspR. In the *B. bronchiseptica* wild-type (upper left), the BspR negative regulation level for the *bsc* locus transcription is moderate, and the T3SS machinery is established. In the Bcr4-deficient strain (upper right), BspR strongly represses the *bsc* locus transcription, and construction of the T3SS machinery is incomplete. In the BspR-deficient strain (lower left), the negative regulatory effect of BspR is cancelled, and the construction of the T3SS machinery is promoted. In the BspR/Bcr4 double-deficient strain (lower right), while the *bsc* locus transcription is promoted because of BspR deficiency, T3SS is not functional.

Fig. S1

bioRxiv preprint doi: https://doi.org/10.1101/2021.09.28.462275; this version posted August 9, 2022. The copyright holder for this preprint (which was not certified by peer review) is the author/funder, who has granted bioRxiv a license to display the preprint in perpetuity. It is made available under aCC-BY 4.0 International license.

```
Bb      1 MHSDSGSDSGSDSGSGS--PMASSIHPSEPIQPMEHVLEEADARLLTEVGFLAAAVSDLT    58
Bp      1 MHSDSGSDSGSDSGSGS--PMVSSIHPSEPIQPMEHVLEEADARLLTEVGFLAAAVSDLT    58
Bpp     1 MHSDSGSDSGSGSGSGSGSPMASSIHPSEPIQPMEHVLEEADARLLTEVGFLAAAVSDLT    60

Bb     59 RADAIFNALQRVRPGRTYPCIGLAVARMNAGLPDEAAEILANFQPAQAEDRSELDAWCGF   118
Bp     59 RADAIFNALQRVRPGRTHPCIGLAVARMNAGLPDEAAEILANFQPAQPEDRSELDAWCGF   118
Bpp    61 RADAIFNALQRVRPGRTYPCIGLAVARMNAGLPDEAAEVLANFQPAQAEDRSELDAWCGF   120

Bb    119 ALLLAGRSDEARRMLQRAIDAGGEAARLAQVVLDSGPAMMRPAPLQSEPLPGAPG        173
Bp    119 ALLLAGRSDEARRMLQRAIDAGGEAARLAQVVLDSGPAMMRPAPLQSEPLPGAPG        173
Bpp   121 ALLLAGRSDEARRMLQRAIDAGGEAARLAQVVLDSGPAMMRPAPLQSEPLPGAPG        175
```

Fig. S2. Alignment of Bcr4 amino acid sequences in representative *Bordetella* species. Bcr4 amino acid sequences of *B. bronchiseptica* S798 (Bb), *B. pertussis* Tohama I (Bp) and *B. parapertussis* 12822 (Bp) were compared using ClustalW. The grey highlighted letters represent amino acid residues that were different from those in Bb. Bcr4 of Bp and Bpp have 98.3% and 97.1% identities with those of Bp, respectively.

Fig. S2

bioRxiv preprint doi: https://doi.org/10.1101/2021.09.28.462275; this version posted August 9, 2022. The copyright holder for this preprint (which was not certified by peer review) is the author/funder, who has granted bioRxiv a license to display the preprint in perpetuity. It is made available under aCC-BY 4.0 International license.

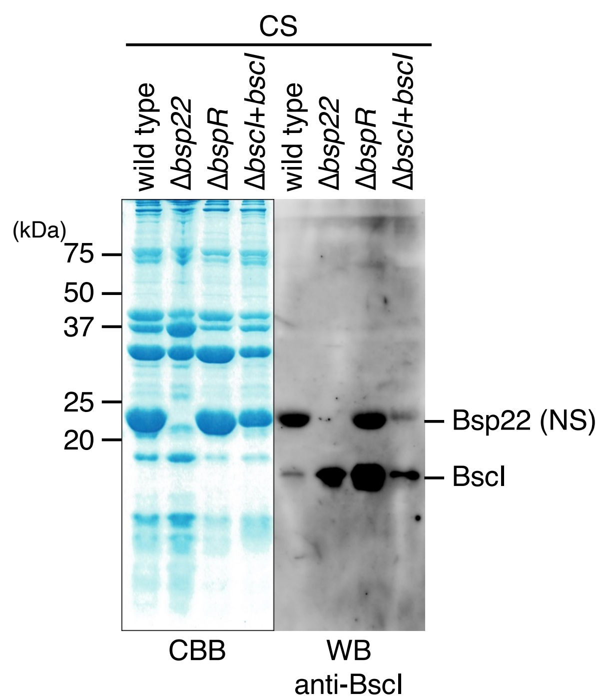

Fig. S3. The nonspecific reaction of anti-BscI antibody to Bsp22. The culture supernatants (CS) were prepared from the wild-type strain, Δ*bsp22* (Bsp22-deficient strain), Δ*bspR* (BspR-deficient strain) or Δ*bscI*+*bscI* (BscI-complemented strain) cultured in SS medium. The CS samples were separated by SDS-PAGE and stained with Coomassie Brilliant Blue (CBB, left panel) or analyzed by Western blotting (WB) with anti-BscI antibody (right panel). NS indicates nonspecific signals. Experiments were performed at least three times, and representative data are shown.

bioRxiv preprint doi: https://doi.org/10.1101/2021.09.28.462275; this version posted August 9, 2022. The copyright holder for this preprint (which was not certified by peer review) is the author/funder, who has granted bioRxiv a license to display the preprint in perpetuity. It is made available under aCC-BY 4.0 International license.

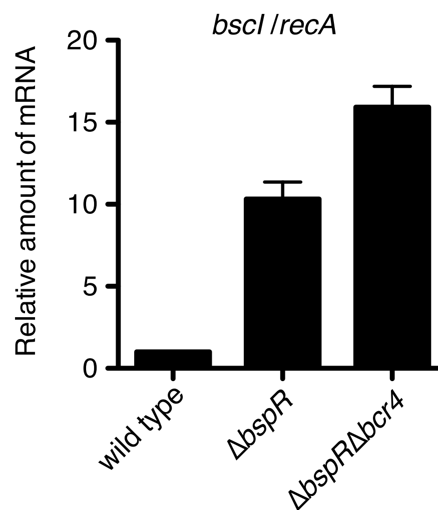

Fig. S4. The results of the RT-PCR analysis for the mRNA level of *bscI* in *B. bronchiseptica* strains. Total RNA was prepared from the wild-type strain, Δ*bspR* (BspR-deficient strain) or Δ*bspR*Δ*bcr4* (BspR- and Bcr4-deficient strain) cultured in SS medium and subjected to a quantitative RT-PCR analysis. The histogram shows the relative amount of *bscI* mRNA normalized by the housekeeping gene, *recA* mRNA. Experiments were performed at least three times, and representative data are shown.

Fig. S4

bioRxiv preprint doi: https://doi.org/10.1101/2021.09.28.462275; this version posted August 9, 2022. The copyright holder for this preprint (which was not certified by peer review) is the author/funder, who has granted bioRxiv a license to display the preprint in perpetuity. It is made available under aCC-BY 4.0 International license.

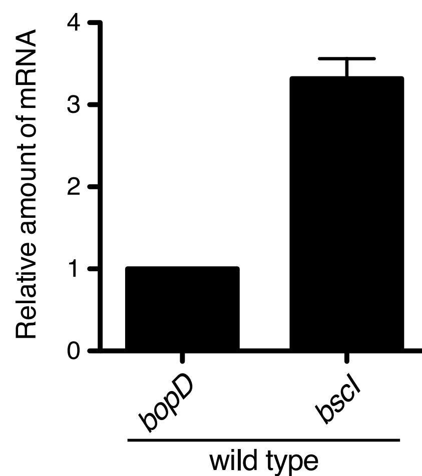

Fig. S5. The results of the RT-PCR analysis for mRNA levels of *bopD* and *bscI* in the wild-type *B. bronchiseptica*. Total RNA was prepared from the wild-type strain cultured in SS medium and subjected to a quantitative RT-PCR analysis. The histogram shows the relative amount of *bopD* and *bscI* mRNA in the wild-type. The relative ratio of *bscI* mRNA is shown when the *bopD* mRNA amount is set as 1. Experiments were performed at least three times, and representative data are shown.

Fig. S5

bioRxiv preprint doi: https://doi.org/10.1101/2021.09.28.462275; this version posted August 9, 2022. The copyright holder for this preprint (which was not certified by peer review) is the author/funder, who has granted bioRxiv a license to display the preprint in perpetuity. It is made available under aCC-BY 4.0 International license.

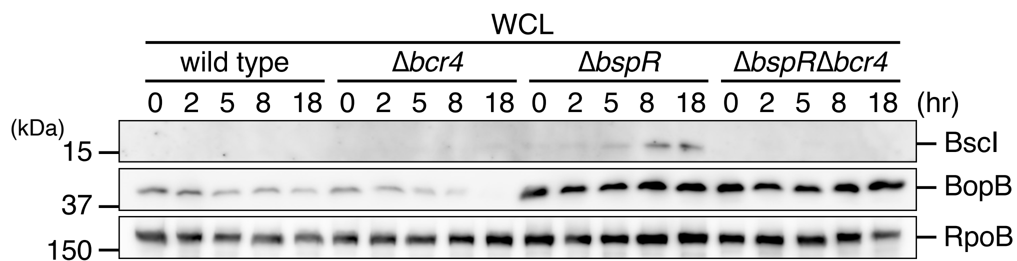

Fig. S6. The time course of BscI production in *B. bronchiseptica*. The whole cell lysates (WCL) were prepared from the wild-type strain, Δ*bcr4* (Bcr4-deficient strain), Δ*bspR* (BspR-deficient strain) or Δ*bspR*Δ*bcr4* (BspR- and Bcr4-deficient strain) cultured in SS medium for 0, 2, 5, 8 or 18 hr. The WCL were separated by SDS-PAGE and analyzed by Western blotting with antibodies against BscI, BopB and RpoB. Experiments were performed at least three times, and representative data are shown.

Fig. S6

bioRxiv preprint doi: https://doi.org/10.1101/2021.09.28.462275; this version posted August 9, 2022. The copyright holder for this preprint (which was not certified by peer review) is the author/funder, who has granted bioRxiv a license to display the preprint in perpetuity. It is made available under aCC-BY 4.0 International license.

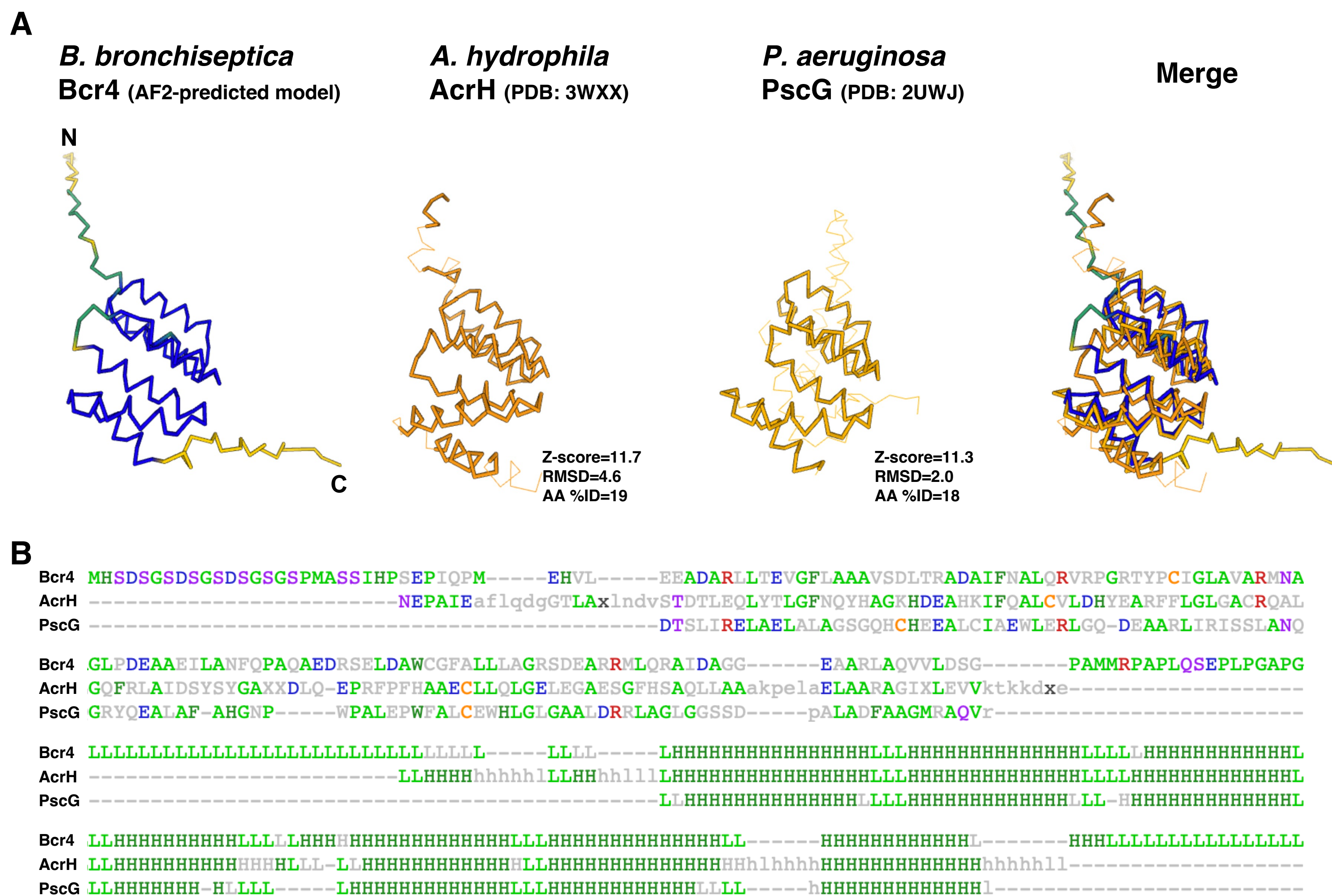

Fig. S7. The predicted structural model of *B. bronchiseptica* Bcr4

(A) The AlphaFold2 (AF2)-predicted structural model of *B. bronchiseptica* Bcr4 and structural comparison with *Aeromonas hydrophil*a AcrH (PDB: 3WXX) and *Pseudomonas aeruginosa* PscG (PDB: 2UWJ). Z-score, root mean square deviation (RMSD), and amino acid identity (AA %ID) of AcrH and PscG compared with Bcr4 are shown, respectively. (B) The pairwise sequence alignment of Bcr4, AcrH, and PscG. The most frequent amino acid type is colored. The secondary structure assignments (H/h: helix, E/e: strand, L/l: coil) are also shown.

Fig. S7